Thermal and Microscopic Investigation of the Unusual Phase Behaviors of Ephedrine Cyclamate

A DISSERTATION

SUBMITTED TO THE FACULTY OF

UNIVERSITY OF MINNESOTA

BY

Arushi Agarwal

IN PARTIAL FULFILLMENT OF THE REQUIREMENTS

FOR THE DEGREE OF

MASTER OF SCIENCE

Changquan Calvin Sun, Advisor

May 2023

Acknowledgments

I would like to wholeheartedly thank my advisor, Dr. Changquan Calvin Sun, for accepting me as a part of his research group and providing this great learning opportunity. He has been an excellent mentor and guide in my research journey. This project would be incomplete without his valuable insights and enthusiasm. I am grateful to him for believing in me and being patient throughout this work. My academic career couldn't have been the same without his guidance. His passion for science is a great inspiration to all of us in the Sun Lab. Dr. Sun's attention to detail leaves me awestruck, and I will try to replicate his approach in my future research. His curiosity and thirst for knowledge have always pushed me to dig deeper into my work. I am grateful to Dr. Sun for creating a constructive working environment and pushing me in the right direction. He has made the Sun Lab a family and helped me build relationships with all my peers. It is a great honor for me to have Dr. Sun as my advisor during this journey toward a master's degree in Pharmaceutics at the University of Minnesota, Twin Cities.

I am grateful to Dr. Raj Suryanarayan and Dr. Christopher Douglas for serving on my master's final examination committee. I appreciate their ideas and constructive comments on my work.

All my well wishes go to the members of the Sun Lab for being my Minneapolis family. Their questions, comments, and discussions helped shape my dissertation and improve my work. I want to especially thank Gerrit Vreeman and Tianyi Xiang for training me with Styl'One and providing their insights to solve the hurdles I faced. I want to thank Dr. Yiwang Guo, Dr. Zhengzheng Zhou, Dr. Chamara Gunawardana, Zijian Wang, Pin-Syuan

Huang, and Yunping Zhoujin for helping me polish my work. I will never forget the scientific discussions we had in the weekly lab meetings, which helped me increase my scientific knowledge. This section would be incomplete without mentioning Vikram Joshi and Vedant Bhagali, who have been my best friends and brothers throughout this journey. They have helped in clearing my doubts, training me, and lending a hand of support whenever needed. I am positive that this is a friendship I am going to cherish all my life.

I also want to thank Dr. Bhushan Munjal, Rahul Lalge, and Jinghan Li for training and allowing me to conduct the DSC and TGA experiments in this dissertation. I would also like to thank Dr. Victor Young and Margaret Clapham for their help with the XRD work and guidance throughout the X-Ray Crystallography course.

I want to thank the Department of Pharmaceutics and the University of Minnesota, Twin Cities, for providing me with the opportunity to pursue my master's degree. In addition, I want to thank Katie James and Amanda Hokanson for their help throughout the two years and for all the fun events they planned for the department. There was never a dull moment at the Dept. of Pharmaceutics in their presence.

My existence would be incomplete without my home and heart, my family. I am eternally grateful to them for always encouraging me to achieve my goals and pushing me in the right direction. My mom has been my ultimate support throughout my life, and no words will be enough to thank her for this life that she gave me. My dad has been the guiding light to my career and has never failed to express his pride in me. I want to thank my sister, Pratika Agarwal, for being my best friend and partner-in-crime since childhood. I would be truly lost and incomplete without her. I am grateful to my grandfather, the late Mr. Nandkishor Lohariwala, for always inspiring me and never letting me feel less of myself. I know that from somewhere, he has been looking out for me. Finally, I want to extend my

gratitude to the rest of my family for always being my pillars of support. I want to especially thank Dr. Anushka Lohariwala for navigating me through life.

I found a home away from home in Minneapolis, and the credit goes to a few very special people in my life. Siddhant Yelwande, Chaitanya Damame, Saahil Samant, Himanshu Joshi, Srujan, Riddhi Kini, and Ketki Pawaskar have been my family thousands of miles away from home, and I am eternally grateful for their presence in my life. I want to thank Wenqi Gai for her friendship, and I can never forget the time I spent with her. I am also grateful to my best friends, Khooshbu Patel and Dhvani Khamar, for never letting me fall.

This journey wouldn't have begun without the blessings of Goddess Saraswati and Lord Krishna. I am eternally grateful for their divine power.

Dedication

To my mom,

Because this was her dream as much as mine

Abstract

Ephedrine is a popular drug used as a bronchodilator and a CNS stimulant. However, it has an extremely bitter taste and very low tabletability. Therefore, a new 1:1 cyclamate salt was formed. The single crystal structure of the new salt was determined using X-ray diffraction, which was called form I. Mechanical analysis revealed that form I is significantly more plastic and exhibits better tabletability than its parent compounds, ephedrine hydrochloride and sodium cyclamate. Thermal analysis proved the existence of another polymorph, form II, which is formed upon heating form I to about 165° C. The two polymorphs are enantiotropically related. DSC revealed that the conversion of form II to I cooling depended on pressure, where it occurred only on cooling a sample heated in a hermetically sealed pan and not in a pan with a pinhole. Attempts were made to produce Form II and understand polymorphism better. However, the phenomenon was preceded by the melting of Form I. Therefore, clear segregation is required between the two processes to understand polymorphism in Eph-Cyc better. The effects of heating rate and crystal size were studied for better optimization. TGA was used as a final attempt to produce Form II using thermal techniques.

Table of Contents

Acknowledgments I
Dedication IV
Abstract V
Table of Contents VI
List of Abbreviations IX
List of Tables X
List of Figures XI
Chapter 1 1
INTRODUCTION 1
1.1 Overview 2
1.2 Crystal Engineering 2
1.3 Cocrystal and Salt Formation 3
1.4 Sweet Crystals and Their Advantages 4
1.5 Ephedrine Hydrochloride 5
1.6 Polymorphism in Crystals 6
Chapter 2 10
PREPARATION AND CHARACTERIZATION OF EPHEDRINE CYCLAMATE 10
2.1 Overview 11
2.2 Introduction 11
2.3 Material and Methods 12
2.3.1 Materials 12
2.3.2 Preparation of single crystals 12

2.3.3 Single crystal X-ray diffraction 12
2.3.4 Powder X-ray diffraction 13
2.3.5 Thermal analysis 13
2.3.6 Dynamic vapor sorption 14
2.3.7 Tabletability 14
2.3.8 In-die P_y analysis 15
2.4 Results and Discussion 15
2.4.1 Single crystal X-ray structure 15
2.4.2 Powder X-ray diffraction 16
2.4.3 Moisture sorption behavior 16
2.4.4 Tabletability and plasticity behavior 16
2.4.5 Thermal properties 17
2.4.6 TGA 1st derivative and TGA of anhydrous sodium cyclamate 17
2.4.7 Key observations and conclusions 18
Chapter 3 31
THERMAL ANALYSIS AND PREPARATION OF FORM II 31
3.1 Overview 32
3.2 DSC Cooling- Reverse Cycle and Enthalpy of Fusion 32
3.3 Pressure-Based DSC Difference 32
3.4 Preparation of Form II: 33
3.5 Hot Stage Results 34
3.5.1 HSM at 165 °C 34
3.5.2 HSM for the melting range of Form I 34
3.5.3 HSM heating rate 35
3.6 TGA Results 35
3.7 Key Observations 36
3.8 Conclusions 36

Chapter 4 49
RESEARCH SUMMARY AND FUTURE WORK 49
4.1 Research Summary 50
4.2 Future Work 50
REFERENCES 51

List of Abbreviations

API	Active Pharmaceutical Ingredient
ODT	Orally Disintegrating Tablets
GRS	Gastro-Retentive System
BCS	Biopharmaceutical Classification System
SPR	Structure Property Relationship
QbD	Quality-by-Design
FDA	Food and Drug Administration
TMP	Tetramethylpyrazine
Na-Cyc	Sodium Cyclamate
Eph-HCl	Ephedrine Hydrochloride
Eph-Cyc	Ephedrine Cyclamate
MW	Molecular Weight
HSM	Hot Stage Microscope
DSC	Differential Scanning Calorimetry
TGA	Thermogravimetric Analysis
RH	Relative Humidity
PXRD	Powder X-Ray Diffraction
DTGA	Derivative Thermogravimetric Analysis
T_m	Melting Temperature

List of Tables

2.1 Crystallographic data for Eph-Cyc 19

2.2 Plasticity parameter for ephedrine HCl, sodium cyclamate, and ephedrine cyclamate from in-die Heckle analysis 20

3.1 Enthalpy of fusion for each transformation step observed in DSC (n = 3) 38

List of Figures

1.1 Energy/temperature diagrams of dimorphic systems; (a)Enantiotropic system, (b)Monotropic system; (Tp: transition point; Tf: fusion point; H: molar enthalpy; G: molar free energy; S: molar entropy; A, B: crystalline modifications; l: liquid phase) 9

2.1 Thin plate-like single crystals of Eph-Cyc under PLM 21

2.2 Crystal structure for Eph-Cyc: (a) Asymmetric unit for Eph-Cyc, (b) Unit cell along a-axis 22

2.3 PXRD patterns for (a) Ephedrine HCl, sodium cyclamate, and ephedrine cyclamate, (b) Experimental and calculated peaks for ephedrine cyclamate 23

2.4 Moisture sorption curve for Eph-Cyc 24

2.5 (a) Tabletability profile, (b) Compressibility profile, (c) Compactibility profile for Eph-Cyc, sodium cyclamate, and ephedrine HCl 25

2.6 HSM images for Eph-Cyc crystals: (a) crystals at room temp, (b) Eph-Cyc begins to transform, (c,d) melting begins for Form II, (e) melt starts to disintegrate, (f) disintegrated melt 26

2.7 DSC curve for Eph-Cyc 27

2.8 (a) TGA curve for Eph-Cyc, (b) TGA 1st derivative curve for the temp range 180° to 220° C 28

2.9 (a) TGA curve for commercial and anhydrous sodium cyclamate, (b) TGA curve for ephedrine cyclamate 29
2.10 Chemical breakdown of cyclamic acid 30

3.1 Cooling curve for DSC of ephedrine cyclamate using a hermetically sealed pan 39
3.2 DSC cooling curve for Eph-Cyc using a pinhole lid 40
3.3 DSC curve for Eph-Cyc before and after introducing an artificial pinhole 41
3.4 Transformation of Eph-Cyc at 160° C 42
3.5 HSM for Eph-Cyc when the temperature is held at 165° C: simultaneous melting and phase transformation can be observed 43
3.6 Attempt at melt crystallization for Eph-Cyc 44
3.7 HSM to determine the melting range of Form I of Eph-Cyc; (a) initiation of melting, (b) melting completed 45
3.8 HSM images of four crystals;(a) melting begins for two crystals, (b)two crystals undergo a transformation, (c) Form I crystals have melted completely, (d) melting of Form II 46
3.9 Phase conversion of Eph-Cyc based on the heating rate 47
3.10 Microscopic images of crystals obtained from TGA; (a,b) crystals stuck in mid-transformation, (c) untransformed crystal (bright pink) along with degenerated crystals (left) 48

Chapter 1

Introduction

1.1 Overview

Pharmaceutical development and manufacturing have become more complicated over the years and require knowledge of various disciplines like biology, medicinal chemistry, material sciences, process engineering, regulatory sciences, and many more [1]. Any drug product needs to be optimized not only according to the active pharmaceutical ingredient (API) but also according to the target population. For example, formulations like suspensions, syrups, and orally disintegrating tablets (ODT) are preferred for non-compliant patients such as infants, toddlers, or even geriatric patients. Many drugs today are also being formulated as gastro-retentive systems (GRS) to reduce the pill load of the patients for better compliance[2]. Thus, it becomes even more critical to understand the drug product's physical and chemical properties thoroughly. Most new APIs today are poorly soluble (BCS class II & IV) and unstable under variable environmental conditions[3,4]. The formulations manufactured for these APIs should compensate for the downfalls of these drugs and provide a long enough shelf life for transport and storage under changing environmental conditions. At the same time, an ideal formulation should be cost-effective and easy to manufacture, package, and transport. Among several approaches available to assist the development of any drug into an ideal formulation is crystal engineering, which is one such approach actively being pursued by researchers across the globe, as it is cost-effective to improve the physical and chemical properties of the drug.

1.2 Crystal Engineering

Crystal engineering is defined as "*The understanding of intermolecular interactions in the context of crystal packing and the utilization of such understanding in the design of new solids with desired physical and chemical properties*" [5]. The basis of this approach lies in the directional and predictable behavior of crystals or supramolecular synthons[6]. These structures can consist of a wide variety of chemical components such as coordination polymers, heavy metals, other APIs, and sugars[6]. The four basic steps of crystal

engineering are: observe structural groups, rationalize crystal packaging, predict, and test the predictions made about these new compounds[7]. Today, researchers from various fields, such as chemistry, material science, and pharmaceutical sciences, are exploring this approach[8].

The crystal engineering approach is commonly used in the pharmaceutical industry to improve the physio-chemical properties of APIs, such as solubility, physical and chemical stability, tabletability, and permeability, without affecting the pharmacological activity[9–13]. Since each multicomponent crystal structure gives a distinct set of mechanical and physiochemical properties, crystal engineering acts as an effective strategy to improve the manufacturability and clinical performance of pharmaceutical products[13,14].

Advancements in X-ray diffraction and crystal structure analysis have made it easier to understand complex intermolecular interactions for establishing a reliable structure-property relationship (SPR) for solids[11]. Accurate SPRs also assist in establishing a better Quality by Design (QbD) approach for pharmaceutical compounds by providing an advanced product and process understanding[14–16]. Major techniques used in crystal engineering are habit modification, surface modification, polymorphism, solvate formation, and cocrystallization and salt formation[17].

1.3 Cocrystal and Salt Formation

Cocrystals are defined as "*Crystals with structure constituted of multicomponent, generally in a stoichiometric ratio, among which one or more components are neutral compounds*"[18]. They broaden the range of solid forms accessible for modulating the pharmaceutical performance appropriate for the desired formulation[13,17,18]. With the increasing relevance of cocrystals in the industry, the United States Food and Drug Administration (FDA) released a guide for the regulatory classification of these pharmaceutical cocrystals[18,19].

Salts are compounds formed from an acid-base reaction, which can either be neutralization (acid-base reaction resulting in the release of water) or proton transfer. Different salts of the same compound are known to exhibit different physical, chemical, and thermodynamic properties. One major factor affecting salt formation is the relative strength of the acid or the base[20]. This was the basis of developing the ΔpKa rule, which states that the possibility of salt formation will significantly increase in cases where ΔpKa is larger than three. A larger ΔpKa facilitates more effortless proton transfer necessary for salt formation[21,22]. In cases where the ΔpKa is lesser than three, the product can either be a cocrystal or a salt [22–24].

Proton Transfer is usually used as a criterion to distinguish salts from cocrystals. But the distinction between salt and cocrystal is not always sharp as proton transfer is not always complete, and it also depends on the temperature and crystal packing[22,25,26]. Cocrystals and salts are similar in terms of definite stoichiometric ratios and solubility, being sensitive to *common-component effects*[27,28]. Therefore, both approaches should be considered to optimize the solid- form of an API to facilitate successful formulation development[18].

1.4 Sweet Crystals and Their Advantages

Most pharmaceutical drugs are bitter, which hinders them from being formulated as chewable tablets, oral suspensions, or solutions. These dosage forms are especially favorable for infants and toddlers[2,18]. Cocrystallization of drugs with artificial sweeteners helps in improving the taste of these formulations. Some commonly used sugar alternates used for cocrystal formation are saccharine, aspartame, acesulfame, sucralose, and cyclamate, which are 30-600 times sweeter than sucrose. Moreover, most sugar alternatives are highly acidic, making them suitable for salt or cocrystal formation with basic drug compounds at molecular level uniformity, further reducing the quantity of sweetener in the formulation to improve the taste profile of the drug.

These sweeteners have also been proven useful in improving the physio-chemical properties of drugs apart from taste masking. For example, sweet salts of tetramethylpyrazine (TMP) with acesulfame and saccharine have a 24% higher bioavailability than the commercially available product[29]. Similarly, berberine salts with acesulfame and saccharine have significantly improved stability and tabletability compared to its chloride salt, which is highly unstable under humid conditions[30]. Tabletability is also significantly improved for sulfamethazine salt with acesulfame[13]. In addition, an orally disintegrating tablet (ODT) formulation was developed using sildenafil acesulfame with improved stability and hygroscopicity[1].

Sodium cyclamate (Na-Cyc) is a salt of cyclamic acid (pKa: 1.71), which was discovered in 1937 by Michael Sveda, a graduate student at the University of Illinois. It is 30-50 times sweeter than sucrose[31]. Cyclamate is resistant to heat and is thus used in food and beverages that require high processing temperatures[32]. However, its use is heavily restricted because of the compound's carcinogenic properties on conversion to cyclohexylamine[32]. Cyclamate has been approved for consumption in over 130 countries, but its use is still highly restricted in the United States and South Korea[33–35].

1.5 Ephedrine Hydrochloride

Ephedrine is a basic drug with a pKa of 13.89. It is derived naturally from the plant *Ephedra sinica* and other members of the same genus and has been actively used in traditional Chinese medicine since 206 BC[36]. Ephedrine hydrochloride (Eph-HCl)came into commercial use by 1926 after being isolated in 1885[36]. Ephedrine acts on the central nervous system and is used in the treatment of bronchial asthma and allergic conditions like urticaria and hypotension. It also has been used as an appetite suppressant and decongestant. It is listed in the pharmacological forbidden substances for doping commissioned by the International Olympic Committee[37]. It is also a schedule 4 substance in the Poisons standard and is only available on prescription[38,39]. It is primarily present in

two chemical forms- ephedrine and pseudoephedrine along with their salts. The two forms are stereoisomers, which are enantiomeric to each other. Both exist in the crystal form $P2_12_12_1$[40–42]. It is also extremely bitter in taste and has low tabletability, and displays considerable table defects, like lamination, when compressed.

1.6 Polymorphism in Crystals

"*Probable every substance is potentially polymorphic. The only question is whether it is possible to adjust the external conditions in such a way that polymorphism can be realized or not" - Maria Kuhnert – Brandstätter*[43,44]

Any chemical compound can contain two kinds of internal structure- crystalline or amorphous. Crystalline materials contain repetitive sequences of the constituent atoms or molecules over the range of six or more unit cells. Periodicity is a classifying trait of crystalline compounds[45,46]. Crystalline compounds exist in various forms, such as solvates, salts, co-crystals, or polymorphs. Polymorphism occurs when the same chemical compound displays two or more different packing arrangements. Different polymorphs are known to exhibit different physical and chemical properties such as solubility, melting point, density, hardness, or stability[47]. A change in environmental conditions, such as temperature and pressure, can induce a polymorphic change. These changes would obey Le Chatelier's Principle; for example, increasing the pressure of the system would lead to the formation of a crystal phase with a reduced volume. The temperature at which polymorphic transformation occurs, the transition point can be compared to the melting point because transformation also includes an exchange of heat and must cross an energy barrier[48]. According to the Gibbs free energy equation, the difference in entropy of the two forms is the energy barrier required to cross for transformation at the transition temperature where the Gibbs free energy of the two forms will be equal.

Polymorphic transition can be classified into two groups- enantiotropic and monotropic. One of the very first definitions of enantiotropy says that for two compounds to be enantiotropic, there needs to exist an equilibrium temperature where one of the two forms is stable below it and the other is stable above [49]. The equilibrium temperature for a monotropic compound either does not exist or exists at a temperature above the melting points of both forms [49]. These two groups can further be described with the help of energy diagrams mentioned in *Figure 1.1*. The Gibbs free energy for enantiotropic systems intersects at the transition temperature, whereas, for monotropic systems, the Gibbs free energy does not intersect below the melting temperatures of the polymorphs. For monotropic systems, even if the environment (temperature or pressure) is modified to temporarily overcome the energy barrier, the system will tend to return to its stable form as soon as the environmental stressors are eliminated.

Based on the thermal behavior of polymorphs, Burger and Ramberger devised four primary rules to differentiate between enantiotropic and monotropic systems.

Heat-of-Transition Rule (HTR) states that above the transition temperature of a system, an endothermic transformation would occur, and the system can be classified as enantiotropic. In the case of exothermic transitions, the system can either be monotropic, or the transition temperature can be higher than the temperature at which the exotherm is seen[50].

Heat-of-Fusion Rule (HFR) states that enantiotropic systems are those where the polymorph with a higher melting point exhibits lower heat of fusion. In contrast, the opposite can be said for monotropic systems. For reactions involving very low heat of transition values, this rule can be the decisive factor in evaluating a polymorphic system as the reliability of DSC in classifying the reaction as endo- or exothermic goes down[50].

The Density Rule (DR) states that at absolute zero temperature, the compound which exhibits higher density will also be the more stable compound. This rule revolves around

hydrogen bonding and its influence on the molecular structure and the density of crystalline compounds. Stronger hydrogen bonding indicates a closer packing giving higher density and stability[50].

Infrared Rule (IR) states that out of the two polymorphic forms, the one with a larger entropy exhibits a higher first absorption band in the infrared spectrum. This rule also primarily applies to hydrogen-bonded crystals, as strong bonds would indicate a higher vibrational frequency. However, extremely sensitive spectrophotometers are required to study the applicability of this rule[50].

HTR and HFR are the two rules that are primarily used to classify polymorphs, as very few exceptions have been discovered for these. DR and IR have more proven exceptions and many compounds have been known to follow a reverse pattern than the one stated in the Infrared Rule[50].

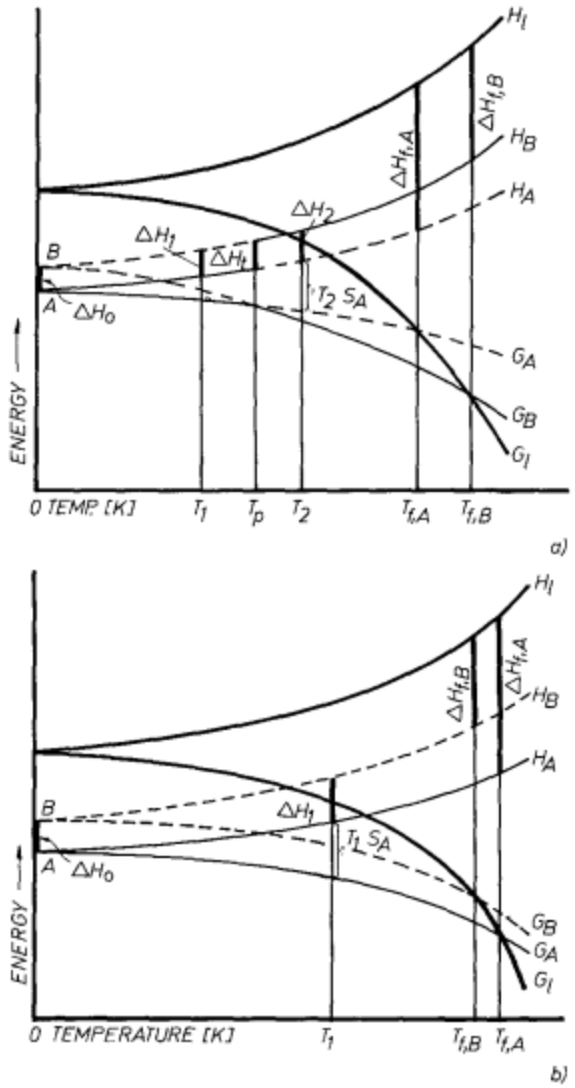

Figure 1.1 Energy/temperature diagrams of dimorphic systems; (a)Enantiotropic system; (b)Monotropic system; (T_p: transition point; T_f: fusion point; H: molar enthalpy; G: molar free energy; S: molar entropy; A, B: crystalline modifications; l: liquid phase)[50]

Chapter 2

Preparation and Characterization of Ephedrine Cyclamate

2.1 Overview

Ephedrine hydrochloride is a CNS stimulant and a bronchodilator. It is highly basic and displays unfavorable physical characteristics such as extremely poor tabletability and bitter taste. An attempt was made to form a sweet salt of ephedrine with cyclamate, which is an acidic compound used as an alternative for sugar in pharmaceutical and confectionery products. The new salt ephedrine cyclamate (Eph-Cyc) was formed by cooling a solution with sodium cyclamate and ephedrine hydrochloride in distilled water. The crystal structure of the new salt was determined using single-crystal X-ray diffraction. The new Eph-Cyc salt displays improved tabletability than Eph-HCl. Thermal analysis reveals that Eph-Cyc is present in at least one polymorphic form, and a transformation can be observed upon heating.

2.2 Introduction

Crystal engineering is a technique used to improve the physio-chemical properties of drug products without altering their biological activity. Drug products are modified to form cocrystals, salts, or even solvates to attain mechanical properties suitable for formulation. Crystal engineering has also been known to improve the stability of APIs under varied temperature and humidity conditions, which helps increase drug product shelf life. The class of sugar alternatives has proved useful for forming cocrystals or salts with APIs. Acesulfame and saccharine have helped improve the bioavailability of tetramethylpyrazine and improve the stability and tabletability of Berberine. Acesulfame has also significantly improved the tabletability of sulfamethazine. Na-Cyc is a sugar alternative that shows high stability at elevated temperatures. It is about 50 times sweeter than sucrose. Cyclamic acid is also highly acidic, with a pKa of 1.71, making it a good candidate for salt formation with basic APIs.

Ephedrine hydrochloride is a bronchodilator and is classified under Schedule 4 for Poisons standard for being a CNS stimulant. It is incredibly bitter and has almost zero tabletability. Ephedrine is also highly basic, with a pKa of 13.89. Based on the large difference between the two ΔpKas, it is predicted that salt formation will occur.

2.3 Material and Methods

2.3.1 Materials

(1S, 2R)-Ephedrine hydrochloride (Sigma Chemical Co, St Louis, MO) and sodium cyclamate (Acros Organics, Geel, Belgium) were used as received.

2.3.2 Preparation of single crystals

Ephedrine hydrochloride (MW- 201.69 g/mol) and sodium cyclamate (MW- 201.22 g/mol) were weighed in an equimolar ratio (0.2 g each) and dissolved in 50 mL distilled water. The suspension was heated while continuously stirred until a clear solution was formed at 72º C. The solution was then covered with parafilm and allowed to cool down slowly. Thin plate-like crystals formed on cooling were filtered using Whatman filter paper *(Figure 2.1)*.

Bulk crystals of Eph-Cyc were prepared using the same technique using approximately 2 g of Eph-HCl and Na-Cyc in 500 ml of distilled water.

2.3.3 Single crystal X-ray diffraction

A single crystal of approximate dimensions of 0.400 x 0.300 x 0.200 mm was isolated and mounted on the tip of a 0.5 mm MiTeGen loop. Data was collected using Apex II diffractometer at 150(2) K. Three sets of 12 frames were harvested from reflections to give a preliminary set of cell constants. The initial orientation matrices were determined from 9883 reflections. The data was collected using MoKa radiation (graphite monochromator), with the detector distance being 6.0 cm and the frame time set at 20 seconds. A resolution of 0.84 Å was used to survey the reciprocal space.

The software packages APEX2, SADABS, and SAINT were used to process data, and the final structure of the crystal was determined using SHELXT 2014/5 and refined using SHELX 2018/3[51]. *P* bca was the assigned space group based on systemic absences and intensity statistics. Direct methods solution provided most non-hydrogen atoms from the E-map. Full matrix least squares /difference Fourier cycles were performed to locate the remaining non-hydrogen atoms. Anisotropic displacement parameters were used to refine all non-hydrogen atoms, and relative isotropic displacement parameters helped place and refine all hydrogen atoms in their ideal positions.

2.3.4 Powder X-ray diffraction

PXRD experiments were carried out on a Powder X-ray diffractometer (PANalytical 16 X'pert pro, Westborough, MA), using Cu Kα radiation (1.54056 Å). The step size for scanning was 0.02° and the dwell time was 1.25 s/step from 5° to 35° 2θ. The tube voltage and amperage were 45 kV and 40 mA, respectively.

2.3.5 Thermal analysis

Hot-stage microscopy (HSM) and polarized light microscopy (PLM) (Eclipse e200; Nikon, Tokyo, Japan) were carried out simultaneously on a single. The crystals were placed in scientifically treated petroleum (STP). The initial experiment was conducted at a 10° C/min heating rate until 250 °C. The later experiments were carried out at varied heating rates of 30, 20, 10, 5, and 2 °C/ min.

The initial differential scanning calorimetry (DSC) (model Q2000, TA Instruments, New Castle, DE) run was performed at 10 °C/min using a hermetically sealed pan using approximately 8 mg of sample. The system was heating till 220 °C. For later runs, different heating and cooling rates were used in the range of 2-30 °C/min. T_{zero} sample pans, with and without a pinhole introduced to an otherwise hermetically sealed lid were used for different runs.

Thermal gravimetric analysis (model Q50 TGA, TA Instruments, New Castle, DE) was conducted using approximately 10 mg of sample in an open aluminum pan with a heating rate of 20 °C/min. The sample was heated to 390 °C.

2.3.6 Dynamic vapor sorption

Water sorption isotherm was determined at 25 °C on an automated vapor sorption analyzer (DVS 1000, Surface Measurement Systems Ltd., Alperton, Middlesex, UK) with continuous 50 ml/min nitrogen flow. The RH values increased from 0% to 50% RH with a step size of 10% and from 50% to 90% with a decreased step size of 5%. The sample was equilibrated at each step until one of the two criteria was met, dm/dt ≤ 0.003% or six h equilibration period.

2.3.7 Tabletability

Eleven tablets were produced using Styl'One Compaction Simulator over a pressure range of 18 – 410 MPa, simulating a Korsch XL 100n at 5 rpm speed. 8 mm tooling was used to produce tablets of approximately 200 mg. The Eph-Cyc powder was crushed using mortar and pestle before compaction. Similar tablets were made for Eph-HCl and Na-Cyc to compare tabletability profiles.

All the tablets produced were diametrically broken with the help of a Texture Analyzer (TA-XT2i; Texture Technologies Corporation, Scarsdale, NY), and the breaking force was recorded. Tensile strength was calculated using:

$$\sigma = \frac{2F}{\pi D h}$$

Where, F = breaking force;

D= tablet diameter;

h= tablet thickness.

The true density of the sample was determined using a helium pycnometer (Quantachrome Instruments, ultra pycnometer 1000e, Boynton Beach, Florida). 1-2 g of the sample was accurately weighed and placed in the sample cell. Measurements were repeated to a maximum of 100, or a <0.005% coefficient of variation of five consecutive measurements were obtained. The reported true density of the sample was the mean of the last five measurements. The true density obtained from the helium pycnometer matched the theoretically estimated true density from the crystal structure.

2.3.8 In-die P_y analysis

The Compaction simulator, Styl'One, was used for data collection with 6 mm tooling with a maximum pressure of 450 MPa. Tablet thickness was measured from the instrument with an accuracy of 1 µm. The tablet weight was measured after ejection. P_y was obtained from a linear regression of the linear portion of the Heckel plot, according to the equation below[52].

$$-ln\,(\varepsilon) = \frac{1}{P_y}P + A$$

2.4 Results and Discussion

2.4.1 Single crystal X-ray structure

Eph-Cyc crystallizes in the orthorhombic *P* bca space group with eight asymmetric units in the unit cell (Z= 8). Each asymmetric unit contains one Eph^+ cation and one Cyc^- anion (Z' = 1). A proton transfer from the sulfamic group of cyclamic acid to the amine group of ephedrine. Each CH_3-N-H^- of ephedrine is connected to two cyclamate molecules (bond length ≈ 2.78 Å). The SO_3^- group of cyclamate is connected to two ephedrine molecules. The third =O of sulfur and -NH group of cyclamate form double hydrogen bonds with -NH and =O of another cyclamate molecule, respectively (bond length ≈ 2.12 Å). The

asymmetric unit and unit cell are shown in *Figure 2.2*. The crystallographic data are shown in *Table 2.1*.

2.4.2 Powder X-ray diffraction

Powder x-ray diffractogram (PXRD) was used to prove the formation of new salt by comparing the diffractogram of bulk Eph-Cyc powder with its parent compounds *(Figure 2.3a)*. PXRD of bulk Eph-Cyc was also compared to the PXRD calculated from the single crystal structure. The PXRD patterns are a good match indicating the phase purity of the sample *(Figure 2.3 b)*. Peak shift was attributed to thermal expansion since the crystal structure was solved at a sub-ambient temperature of 150 K.

2.4.3 Moisture sorption behavior

High hygroscopicity is an undesirable property for pharmaceutical compounds as it hinders manufacturing by altering the stability, tabletability, and flow[53–55]. Ephedrine free-base can form a hemihydrate in highly humid conditions[56]. Cyclamic acid is stable and does not exhibit hygroscopicity[57]. Eph-Cyc also exhibits low hygroscopicity, with its moisture uptake ≤0.8% at RHs up to 95% *(Figure 2.4); thus*, more preferred over ephedrine free-base in terms of physical stability against high humidity.

2.4.4 Tabletability and plasticity behavior

Ephedrine cyclamate displays improved tabletability than Eph-HCl and Na-Cyc till 300 MPa compaction pressure. Above 300 MPa, Eph-Cyc tablets undergo over-compression and show reduced tensile strength. Eph-HCl displays almost zero tabletability since intact tablets free from visible lamination could not be prepared, even at high pressures. The tabletability of Eph-Cyc is still low against the industrially accepted standard for tensile strength 2MPa[58], but it is higher than both its parent compounds *(Figure 2.5a)*. This can also be correlated with the lower P_y value of Eph-Cyc, suggesting higher plasticity than the two parent salts *(Table 2.2)*. The compressibility and compactibility curves of Eph-Cyc are

too scattered to curve fit. The improved tabletability is attributed to the better compressibility of Eph-Cyc than Na-Cyc since there is no significant difference in their compactibility profiles.

2.4.5 Thermal properties

HSM results indicated a solid-state polymorphic change at 170 ℃ followed by melting at 175 °C, which was immediately followed by degradation of the compound *(Figure 2.6*). These were corroborated by the DSC data, where two endothermic peaks are shown at 165 °C and 182 °C immediately followed by an exotherm (*Figure 2.7*). This data suggested the possibility of a polymorphic phase transition before melting.

2.4.6 TGA 1st derivative and TGA of anhydrous sodium cyclamate

The TGA graph indicated a slight weight loss at 200 ℃ of about 1.2% *(Figure 2.8b*). As the temperature increased above 260 ℃, the % of weight loss reached more than 80% (Figure *2.8a*). The close similarity in the first derivative TGA (DTGA) curves of anhydrous Na-Cyc and Eph-Cyc in the 250-350 ºC range suggests the same weight loss mechanism, which was shown for anhydrous Na-Cyc. There seems to be a dissociation of the salt upon melting to form cyclamic acid (immediately converted to N, N'- dicyclohexylsulfamide) and ephedrine free-base at 200 °C (*Figure 2.9*). N, N'- dicyclohexylsulfamide further disintegrates at approximately 280 °C to form oxides of calcium, sulfur, and nitrogen, (*Figure 2.10)*[59]. By analogy, we interpret the weight loss of Eph-Cyc as dissociation upon melting at 180 ºC to form cyclamic acid and ephedrine free-base, with the first loss attributed to sublimation of ephedrine and sulfuric acid (Figure 2.10). N, N'- dicyclohexylsulfamide undergoes thermal degradation at approximately 280 ºC to give the second weight loss curve.

2.4.7 Key observations and conclusions

A new ephedrine cyclamate salt was produced using Eph-HCl and Na-Cyc. X-Ray diffraction was used to prove the formation of a new salt, and its crystal structure was established. Eph-Cyc has significantly lower hygroscopicity than ephedrine free-base; thus, it is more suitable for tablet manufacturing. Eph-Cyc displayed better mechanical properties than its parent compounds regarding tabletability and plasticity. Thermal analysis revealed that Eph-Cyc exists in at least two polymorphic forms. The salt also dissociates on melting to form ephedrine free-base and cyclamic acid.

Table 2.1 Crystallographic data for Eph-Cyc

Name	**Eph-Cyc**
Formula	$C_{16}H_{28}N_2O_4S$
Formula weight	344.46
Temperature / K	150 (2)
Crystal system	Orthorhombic
Space group	*P* bca
a, Å	9.3623 (3)
b, Å	14.4869 (4)
c, Å	26.0845 (7)
a, deg	90
b, deg	90
c, deg	90
Volume, $Å^3$	3537.86 (18)
Z	8
Dc/g cm^{-3}	1.293
F (000)	1488
GOF	1.007
R1 [I>2sigma(I)]	0.0326
wR2 [I>sigma(I)]	0.0912

Table 2.2 Plasticity parameter for Eph-HCl, Na-Cyc and Eph-Cyc from in-die Heckle analysis

	P_y (MPa)
Sodium cyclamate	108.3 ± 4.7
Ephedrine HCl	86.8 ± 2.4
Ephedrine cyclamate	62.4 ± 1.4

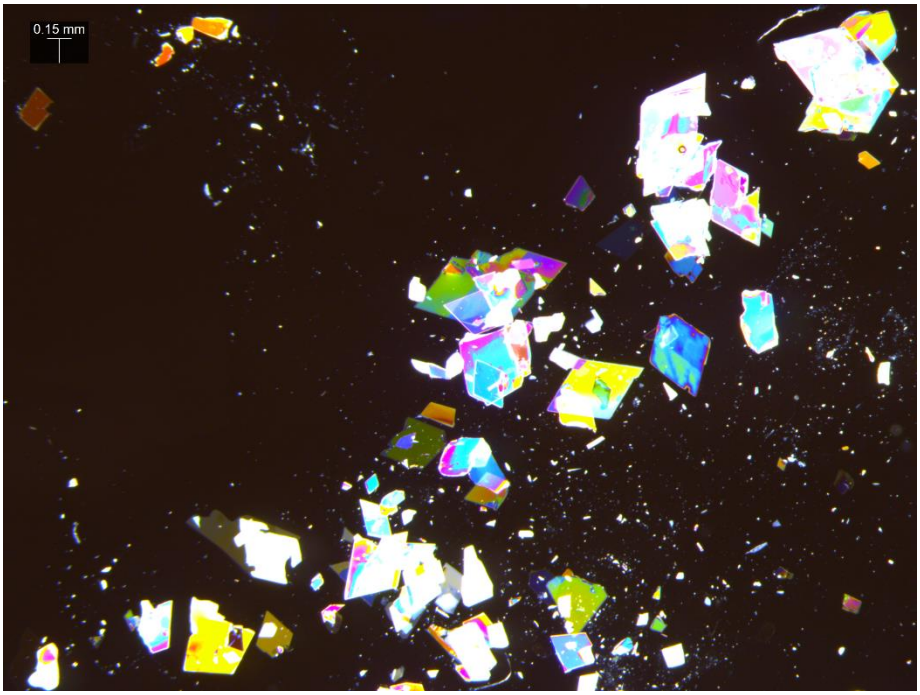

Figure 2.1 Thin plate-like single crystals of Eph-Cyc under a polarized light microscope

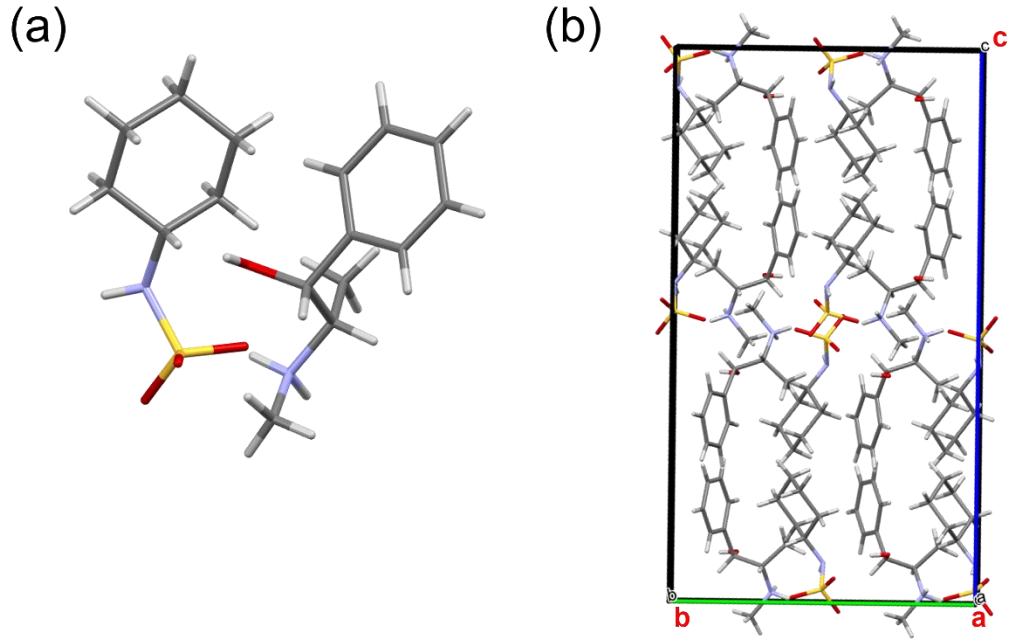

Figure 2.2 Crystal structure of Eph-Cyc: (a) Asymmetric unit; (b) Unit cell view along the a-axis

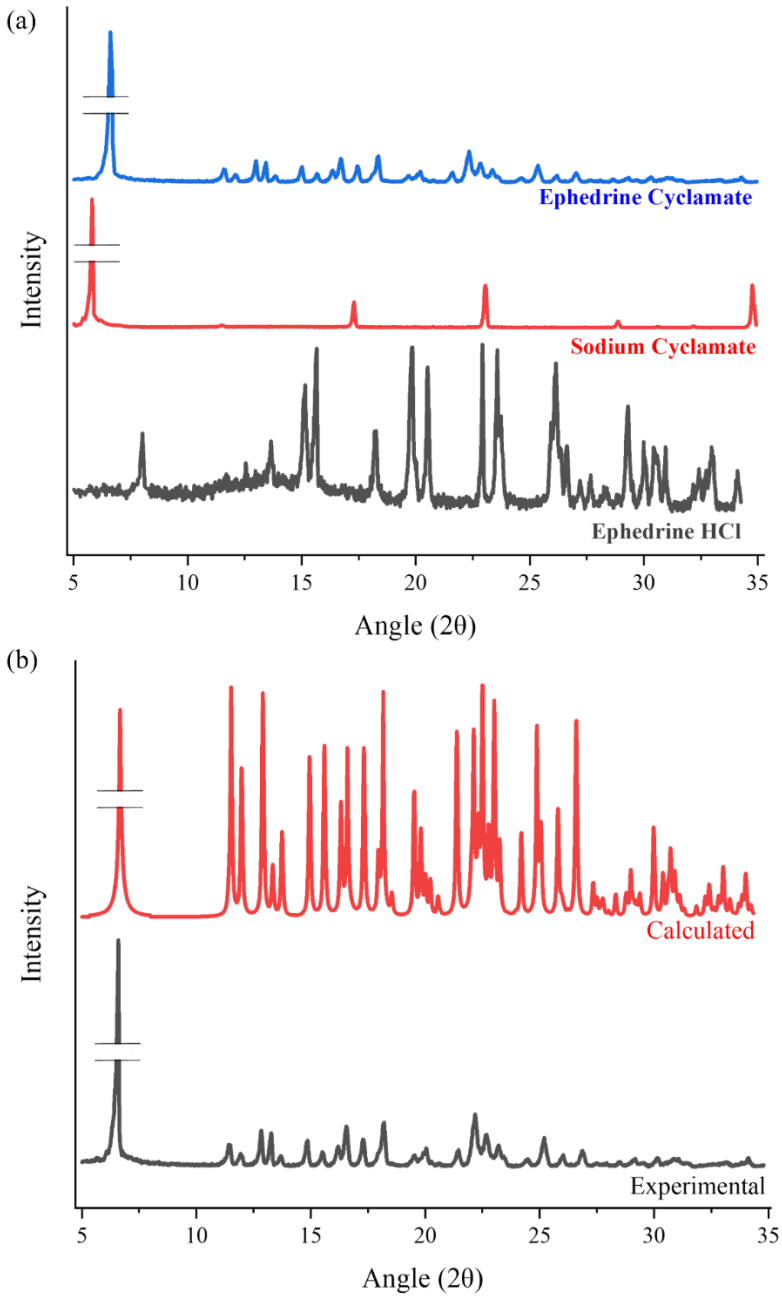

Figure 2.3 PXRD patterns for (a) Eph-HCl, Na-Cyc, and Eph-Cyc, (b) Experimental (298 K) and calculated patterns (150 K) for Eph-Cyc

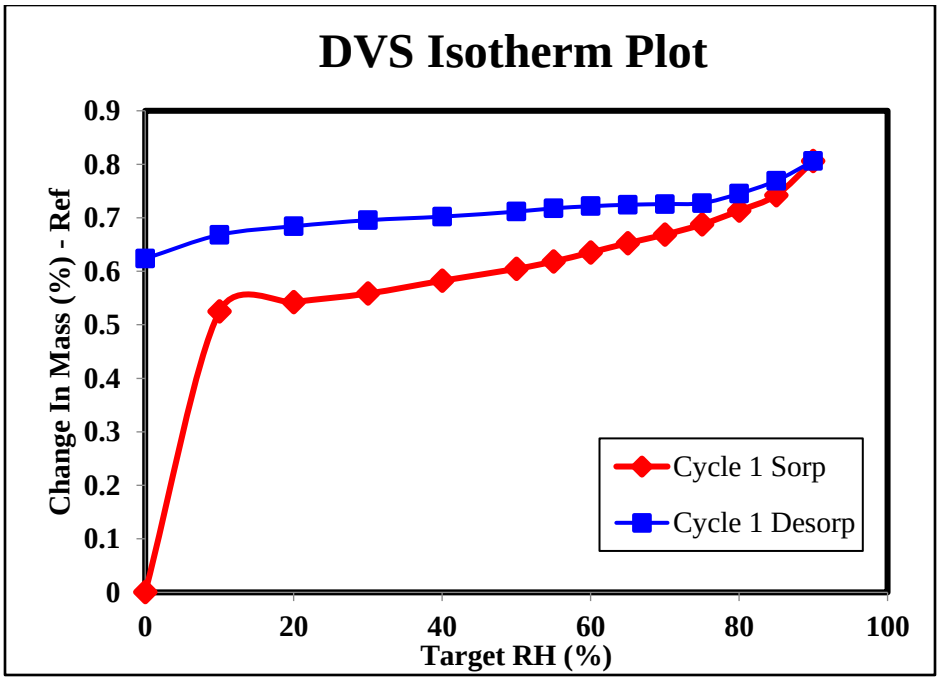

Figure 2.4 Moisture sorption curve of Eph-Cyc

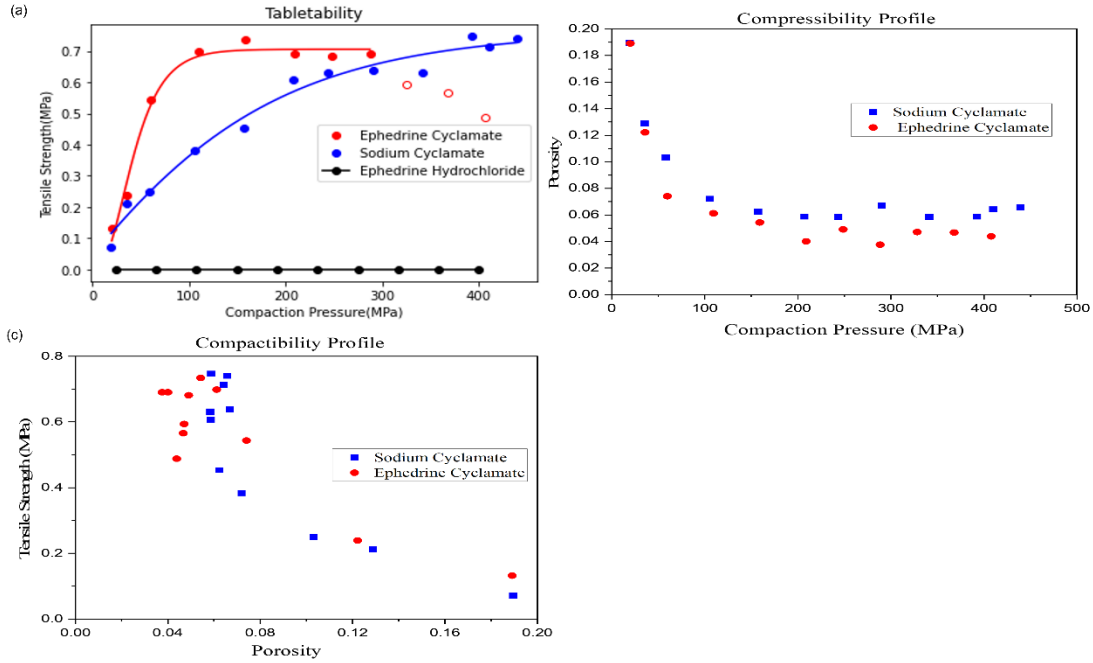

Figure 2.5 (a) Tabletability profile, (b) Compressibility profile, (c) Compactibility profile of Eph-Cyc and Na-Cyc. Eph-HCl failed to form intact tablets.

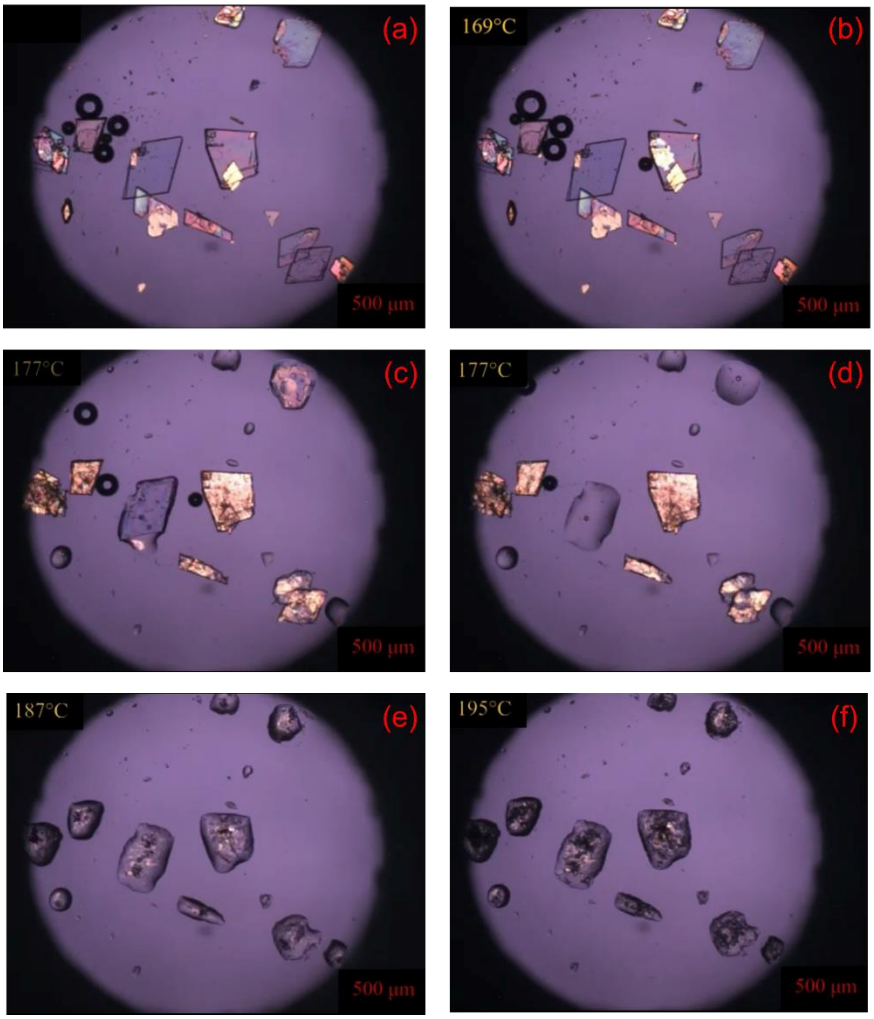

Figure 2.6 HSM images for Eph-Cyc crystals: (a) crystals at room temp, (b) Eph-Cyc begins to transform, (c,d) melting begins for Form II, (e) melt starts to disintegrate, (f) disintegrated melt

Video link:
https://drive.google.com/file/d/1bqd2m21ZQtQxVxLBCMFOVUT_iiqXqW3F/view?usp=share_link

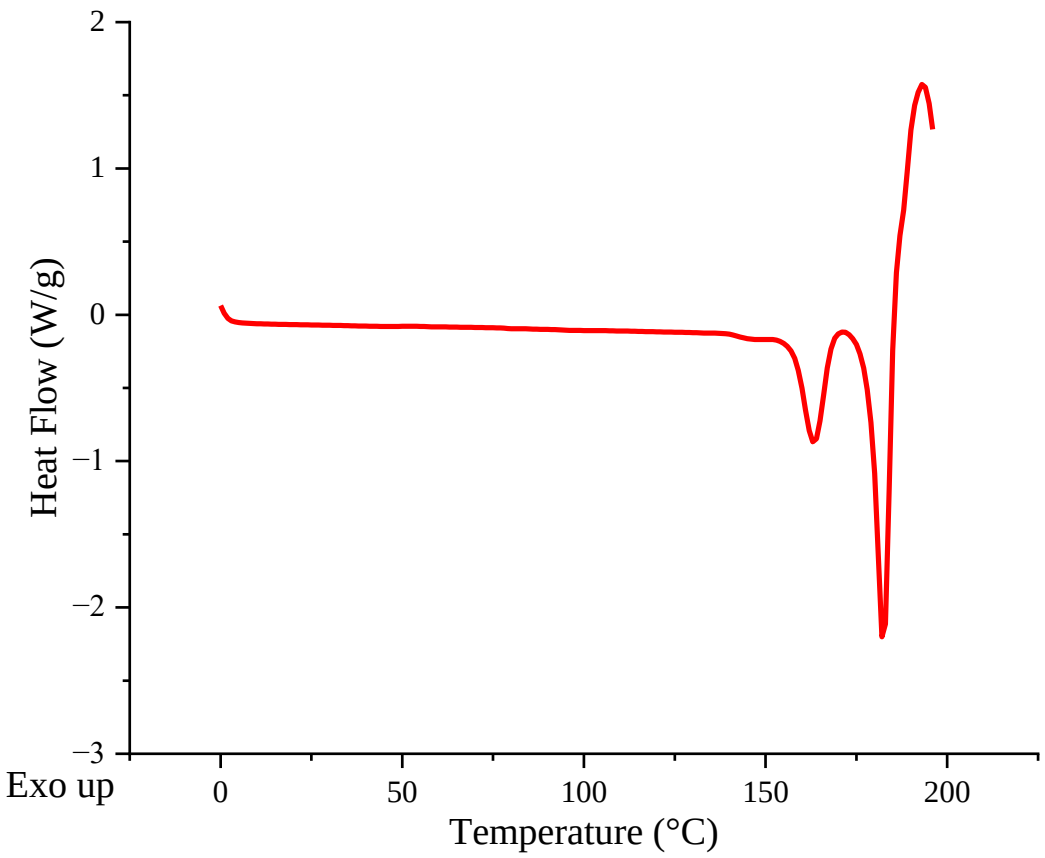

Figure 2.7 DSC curve for Eph-Cyc

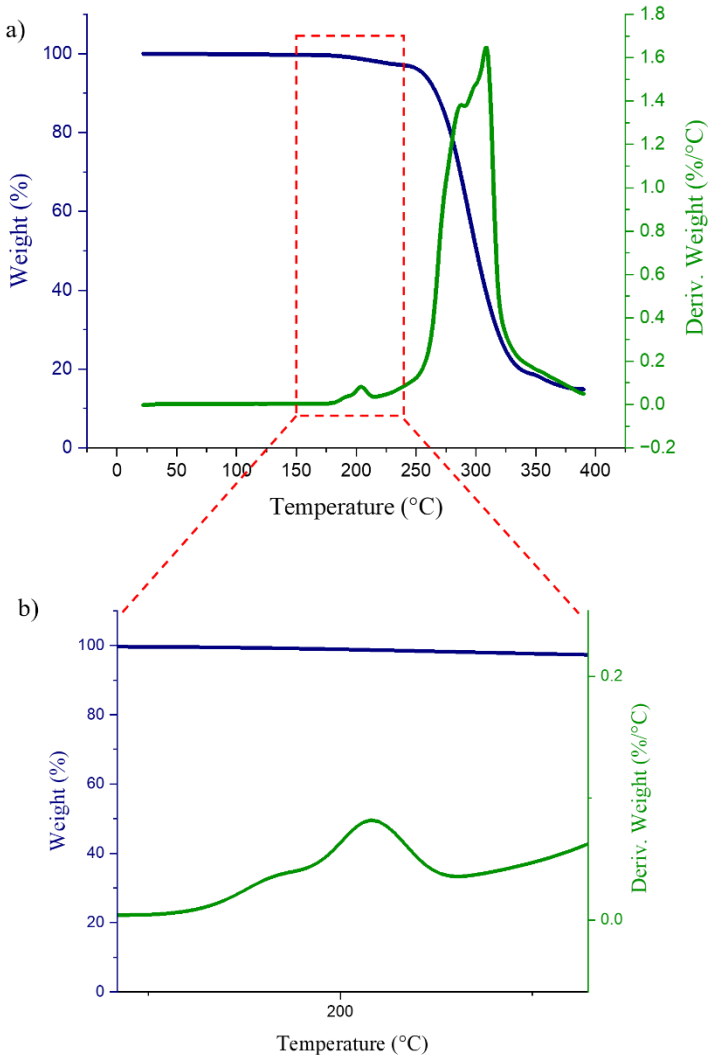

Figure 2.8 (a) TGA curve for Eph-Cyc, (b) TGA 1st derivative curve for the temperature range 180° to 220° C

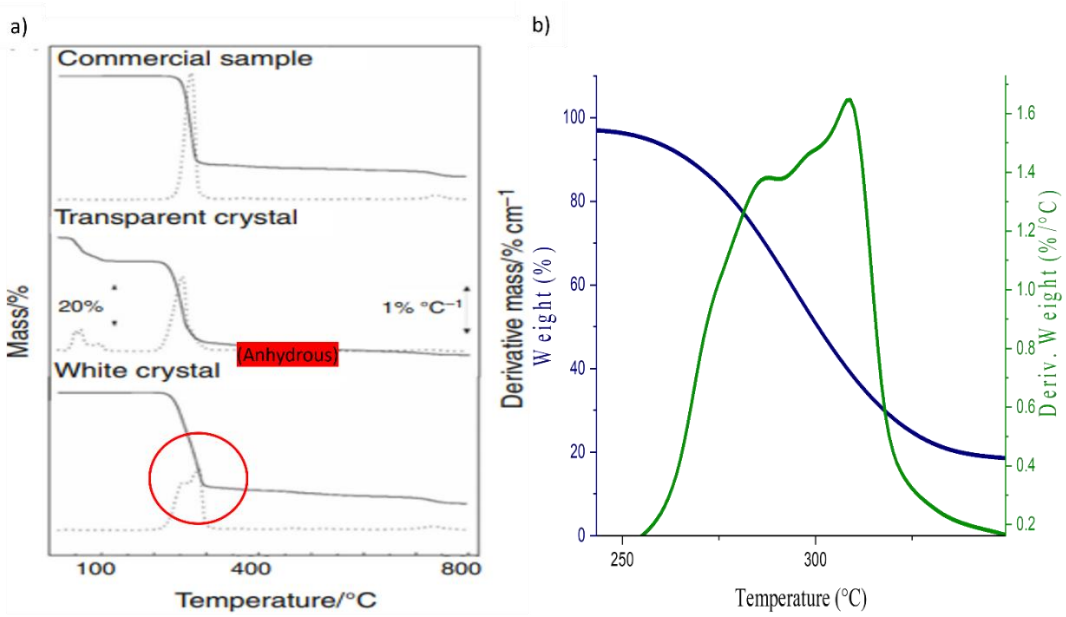

Figure 2.9 (a) TGA curve for commercial, hydrate and anhydrous Na-Cyc [59], (b) TGA curve for Eph-Cyc

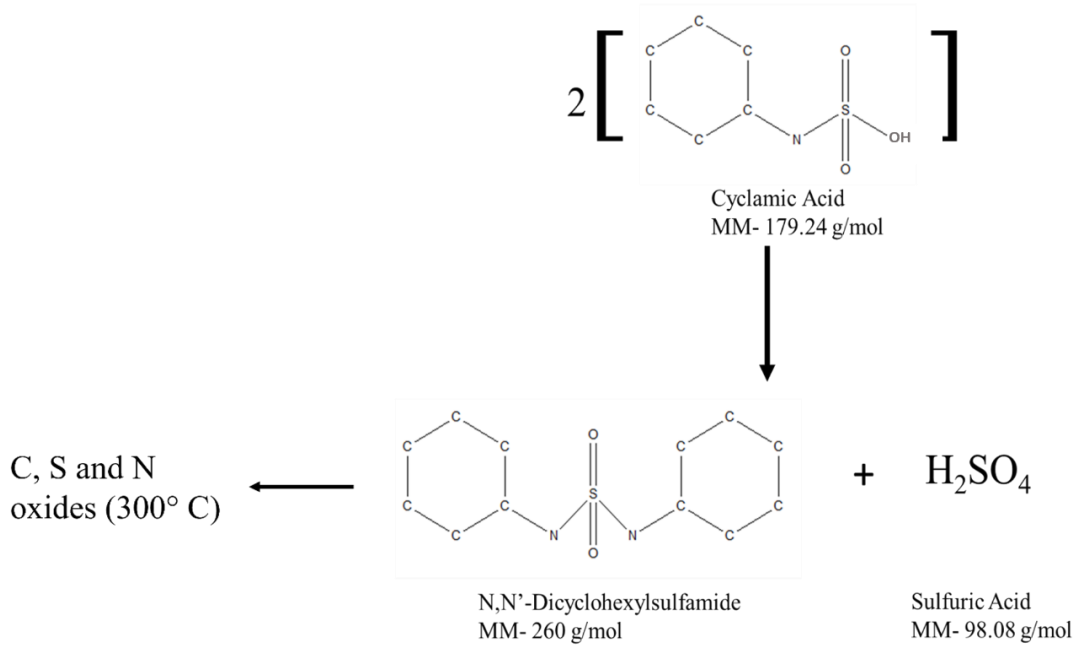

Figure 2.10 Chemical breakdown of cyclamic acid when heated[59]

Chapter 3

Thermal Analysis and Preparation of Form II

3.1 Overview

Further thermal analysis was carried out on Eph-Cyc to better understand the conversion between the two polymorphs. DSC was the primary tool for experimentation during this phase of the project. Some unexpected results were observed in DSC during the cooling stage, which are explained below.

3.2 DSC Cooling- Reverse Cycle and Enthalpy of Fusion

The DSC experiment was repeated in a hermetically sealed pan, where a sample was heated to about 175 °C before cooling to room temperature. Then, the sample was reheated till 220 °C. The whole run was carried out at 10 °C/min.

Upon cooling, an exotherm was observed at 47 °C, whose enthalpy was similar to the enthalpy of fusion of the first endotherm upon heating (*Table 3.1)*. Upon reheating the sample, Eph-Cyc followed a similar pattern, i.e., two endotherms followed by an exotherm. The only difference is that the first endotherm shifts to a lower temperature of about 150 °C. However, the melting endotherm remains constant (peak at 182 °C)

From the above observations, it can be concluded that the two Eph-Cyc polymorphs undergo a reversible phase transformation. Form II converts back to Form I (original form) on cooling corresponding to the exotherm at 47 °C. The shift in the form I to form II transformation temperature during re-heating can be explained by the crystal defects introduced in the sample during the first heat-cool cycle. Upon reheating, the enthalpy of the phase transformation from Form I to Form II matches the enthalpy during the first heating.

3.3 Pressure-Based DSC Difference

The above experiment of the heat-cool cycle for DSC was repeated with two kinds of DSC lids. One with a hermetically sealed system (*Figure* 3.1) and the other with a pinhole lid (*Figure* 3.2).

A reversible phase transition occurs on cooling in a hermetically sealed pan but is absent with a pinhole lid. The pressure elevation in the sealed pan, by the release of residual moisture or sublimation of ephedrine, is attributed to this phenomenon. When a pinhole lid was used, the salt displayed a similar endothermic phase transition curve on the first heating but directly undergoes melting and dissociation (T_m: 182 °C) on the second heating, which is consistent with the absence of conversion back to form I upon cooling.

To prove this hypothesis, another experiment was carried out where the first heat-cool cycle was carried out in a hermetically sealed pan. After cooling, the DSC curve was observed to view the exotherm transformation to Form I. However, an exotherm on cooling was absent when the same sample was heated and cooled using the same parameters when a pinhole was introduced to the same DSC pan using a needle to relieve any pressure buildup (*Figure 3.3)*. Thus, the Form II polymorph remains stable when cooled to room temperature if a pressure buildup in the DSC pan is avoided.

The run was also repeated with a hot stage, where a single crystal of Eph-Cyc of about 2 mm was heated to 160 °C, and the temperature was held until phase transition occurred. On cooling to room temperature, the crystal did not exhibit any change that is indicative of polymorph phase change (*Figure 3.4b)*.

4.1 Preparation of Form II:

Till now, there is very little information about the Form II of Eph-Cyc. From the above experiments, it is known that Eph-Cyc transitions at about 160 °C and does not exhibit reverse transformation on cooling under atmospheric pressure. Thus, it should be possible to prepare bulk form II by heating and cooling if pressure buildup is avoided, following the conditions employed in the DSC experiment. However, as discussed below, this turned out to be difficult to achieve.

5.1 Hot Stage Results

All the previous experiments on the HSM resulted in a visible phase transition. However, the crystals obtained were polycrystalline in nature and were not fit for single-crystal X-ray diffraction. Therefore, attempts were made to obtain single crystals of Form II by modifying the parameters of the hot stage and controlling the crystal size.

Attempts were also made to form single crystals using the melt crystallization technique. But since the salt dissociates upon melting, as observed in section 2.4.6, recrystallization of Eph-Cyc was not possible. This observation is evident in *Figure 3.5*, where a partially molten crystal only solidifies without showing any sign of recrystallization upon cooling to room temperature. Another interesting observation in Figure 3.5 is melting of Form I crystal precedes phase conversion. Thus, it is possible to determine the melting point of Form I.

3.3.1 HSM at 165 °C

It is known that the solid-state transition of Form I to II on hot-stage begins at 165 °C. Therefore, to obtain good single crystals of Form II, it was hypothesized that holding crystals at the onset temperature would lead to the formation of better-quality form II crystals. Hence, HSM runs were designed to hold the temperature at 165 °C (10 ºC/min) for about 10 min using crystals about 1 mm in size.

The run again displayed the melting of Form 1 followed by solid-state phase transformation in the same crystal (Figure *3.6)*. To better separate the two melting and phase conversion processes, different heating rates and crystal sizes were systematically varied.

3.3.2 HSM for the melting range of Form I

Smaller crystals would tend to favor melting over phase transformation due to fewer crystal defects, which leads to slower solid-state polymorph conversion kinetics. Hence, to determine the melting range of Form I of Eph-Cyc, four crystals of about 200 µm were

heated from 145 °C at a rate of 2 °C/min under HSM. All four crystals in *Figure 3.7a* melted without any sign of transformation in the temperature range of 150 to 165 °C *(Figure 3.7b*).

From Chapter 2 of this work, the melting of Form II of Eph-Cyc ranged 172 to 185 °C. A gap of about 10-15 °C exists between the melting ranges of the two polymorphic forms. This was also confirmed with the help of a hot stage microscope, as shown in *Figure 3.8*, where four crystals of 200-300 µm were observed under a heating rate of 20 °C/min. Two crystals converted to form II, while the other two crystals melted. The form II crystals remain solid after the complete melting of form I (Figure *3.8c*). The melting temperature range of form I is 150 to 160 ºC, whereas the melting temperature of form II is 182 ºC which is consistent with the melting temperature measured by DSC (Figure 2.7).

3.3.3 HSM heating rate

Hot-stage experiments were repeated using varied heating rates to identify suitable conditions for reliably observing the transformation of Form I crystals to Form II, assuming that a lower heating rate would favor melting. The heating rates of 2, 10, 15, 20, 25, and 30 °C/min were used to heat single crystals of 100-200 µm, and it was observed that the probability of phase transition was the highest when the heating rate was 15-25 °C/min. In fact, none of the crystals converted to form II at heating rates of 2 and 10 ºC/min, while only 25% of crystals converted at 30 °C/min *(Figure 3.9)*.

3.4 TGA Results

From the above experiments, it is evident that hot-stage is not effective for obtaining form II crystals for bulk characterization. It is possible that crystal form change is extremely sensitive to temperature, which may differ between HSM and DSC. Thus, heating Eph-Cyc in TGA might provide temperature control closer to that in DSC, and, hence, it may

be possible to prepare enough bulk form II (approximately 50 mg) for further characterization, e.g., by PXRD.

However, even with TGA, the transition was not uniform, where some crystals underwent degeneration (*Figure 3.10c),* while others were stuck in mid-transition (*Figure 3.10a &b*) or completely converted to polycrystalline Form II, as observed previously. In addition, a few crystals remained untransformed *(Figure 3.10c).* A sample was held at 165 °C for 15 minutes to ensure complete phase conversion. All the crystals underwent melting and formed a solid mass. When the hold time was reduced, similar results were observed, though to a less extent.

3.5 Key Observations

In this section, we proved the existence of two enantiotropic polymorphs with a transition temperature that lies between 47 ºC and 155 ºC using cooling DSC and HSM.

An interesting observation was the effect of pressure on polymorphic transition behavior. Form II to I conversion occurred under a pressurized atmosphere on cooling, but absent if the pressurization of the sample can be avoided. Although, this suggests a simple way to prepare bulk form II, our efforts were futile due to a rather unpredictable phase change of form II to form I during heating under various conditions.

3.6 Conclusions

Ephedrine cyclamate crystallizes in the form of white plate-like crystals from distilled water. The structure of Eph-Cyc was determined, and the crystals exist in the *P* bca space group. The PXRD patterns were compared to confirm the formation of a new compound. Eph-Cyc shows significantly improved mechanical properties as compared to Eph-HCl, in terms of tabletability and hygroscopicity. Thermal analysis revealed that the form I salt transforms into another polymorphic form on heating it to approximately 165 °C before dissociating into ephedrine free base and cyclamic acid upon melting. The two polymorphs

are enantiotropically related with the transition temperature lying between 47 °C and 155 °C. The conversion of form II to form I on cooling exhibits unusual sensitivity to atmospheric pressure, and it only takes place under hermetic conditions during DSC.

Form I to II conversion of Eph-Cyc is unpredictable and non-uniform, which prevented the preparation of bulk form II powders for more detailed characterization.

Table 3.1 Enthalpy of fusion for each transformation step observed in DSC (n = 3)

Step	Enthalpy of fusion (J/g)
Form I to Form II	44.4 ± 2.4
Form II to Form I	37.3 ± 5.5
Form II melting	96.3 ± 6.3
Form II dissociation	146.5 ± 1.9

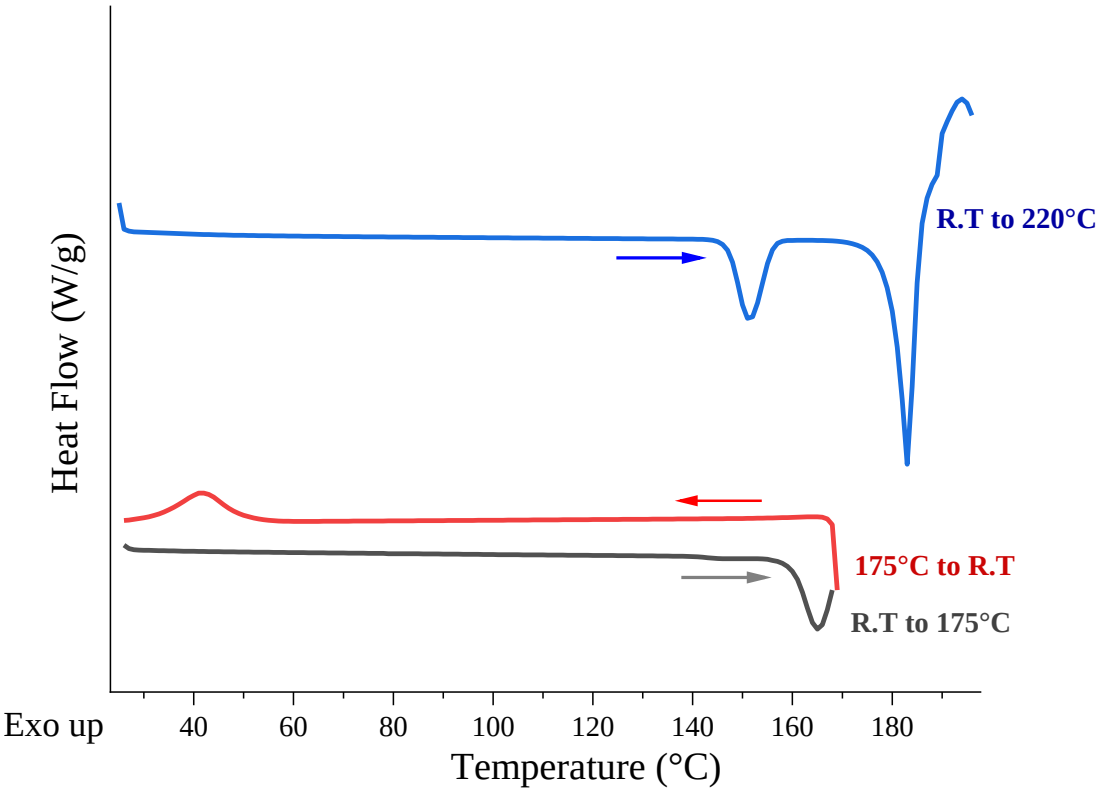

Figure 3.1 Cooling curve for DSC of Eph-Cyc using a hermetically sealed pan

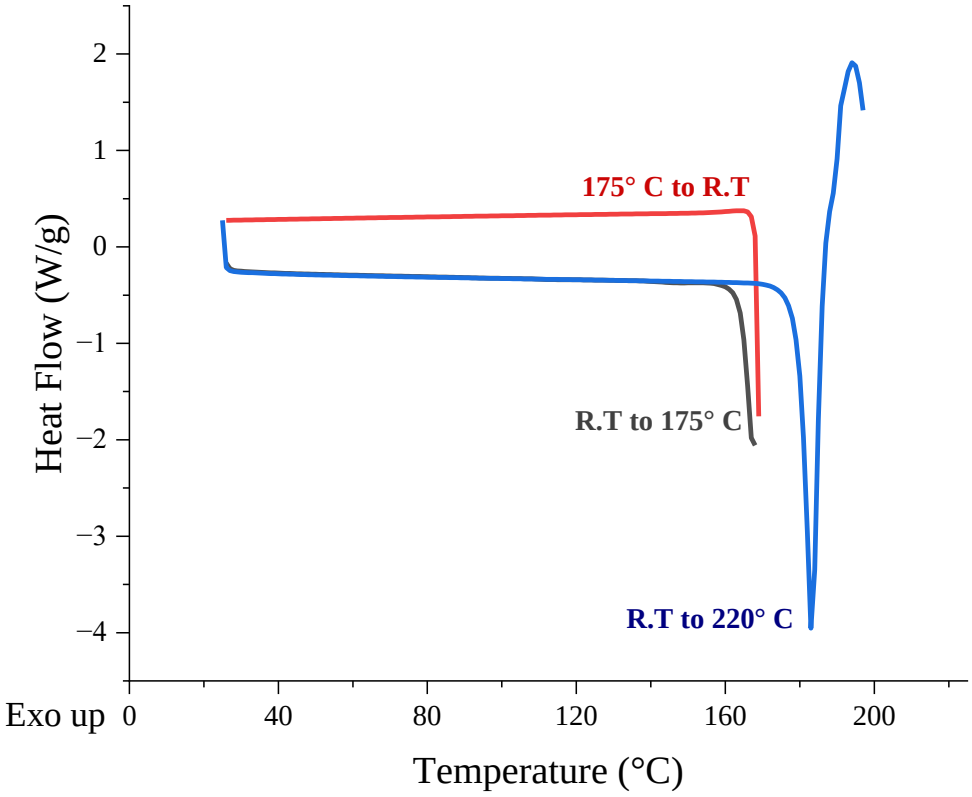

Figure 3.2 DSC cooling curve for Eph-Cyc using a pinhole lid

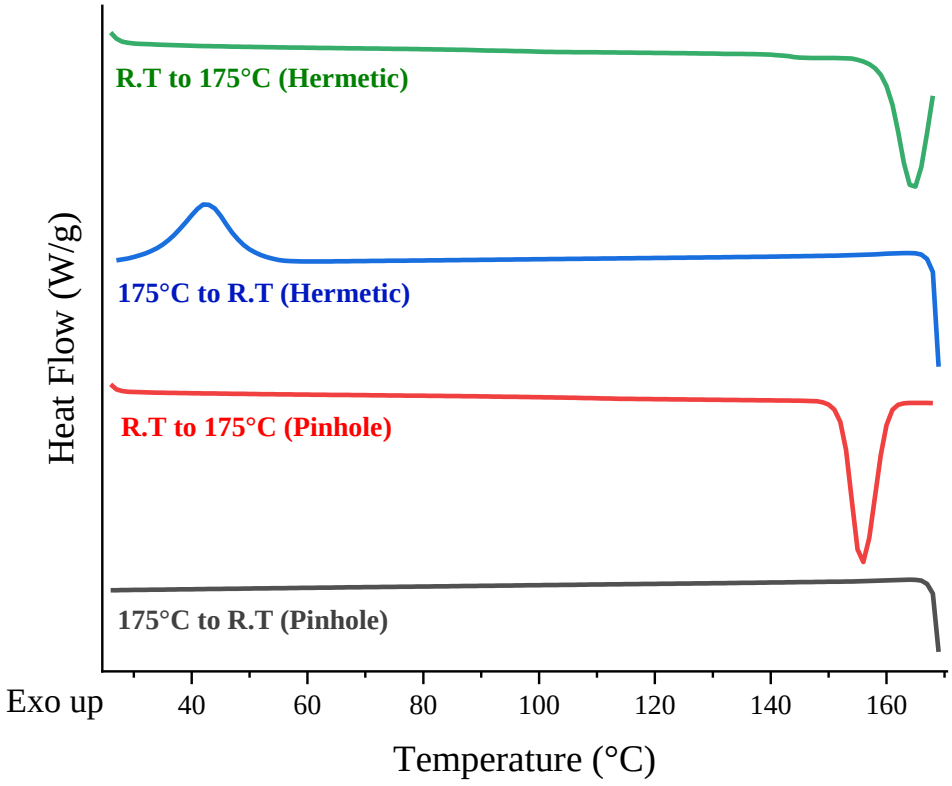

Figure 3.3 DSC curve for Eph-Cyc before and after introducing an artificial pinhole

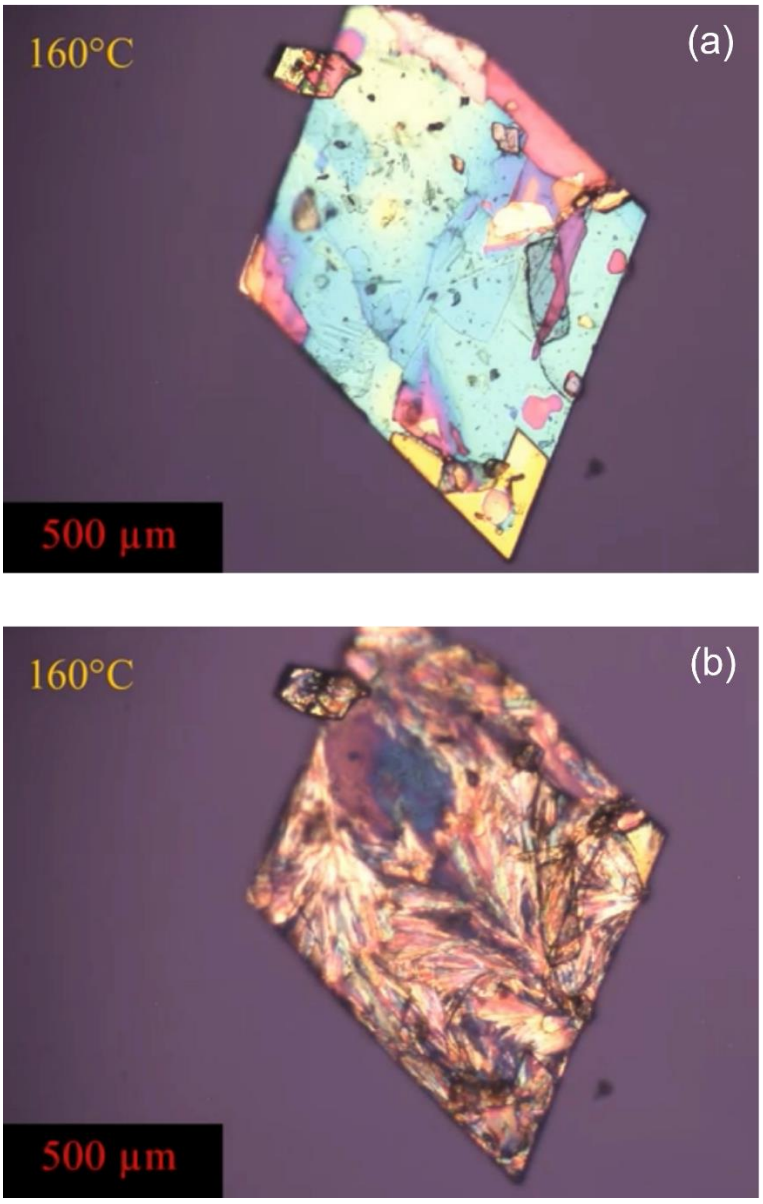

Figure 3.4 Transformation of Eph-Cyc at 160 °C

Video link:

https://drive.google.com/file/d/1hSXUFHlFdCuC82xAVIr_xxf2lOcFfovP/view?usp=share_link

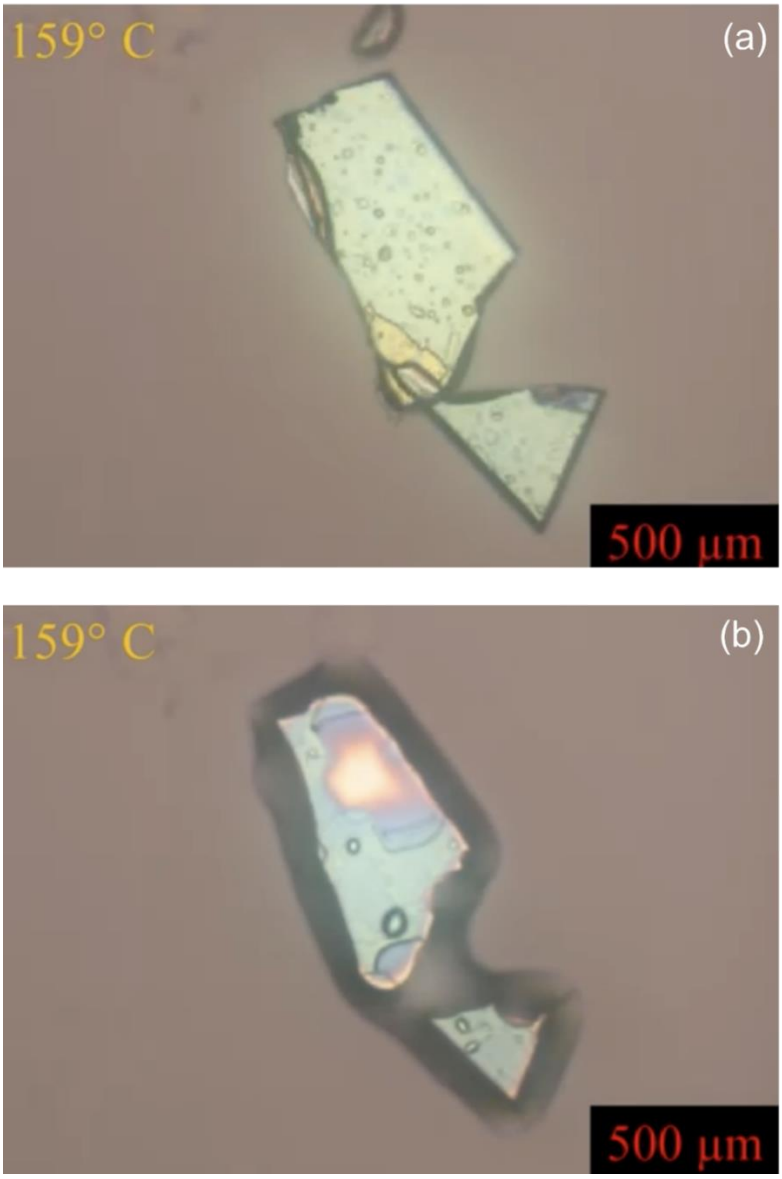

Figure 3.5 Attempt at melt crystallization for Eph-Cyc

Video link:

https://drive.google.com/file/d/1eez1FIJcZL9Tkc9_k2cdK-gBrB9p24zB/view?usp=share_link

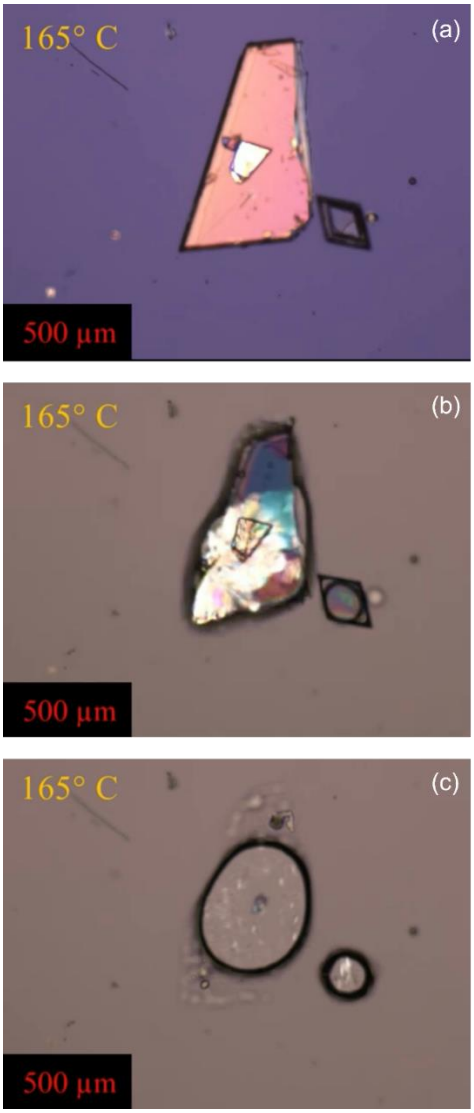

Figure 3.6 HSM for Eph-Cyc when the temperature is held at 165° C: simultaneous melting and phase transformation can be observed

Video link:

https://drive.google.com/file/d/1abcV-DiA2nEQXSIagXdN0gA4fU5VZvgP/view?usp=share_link

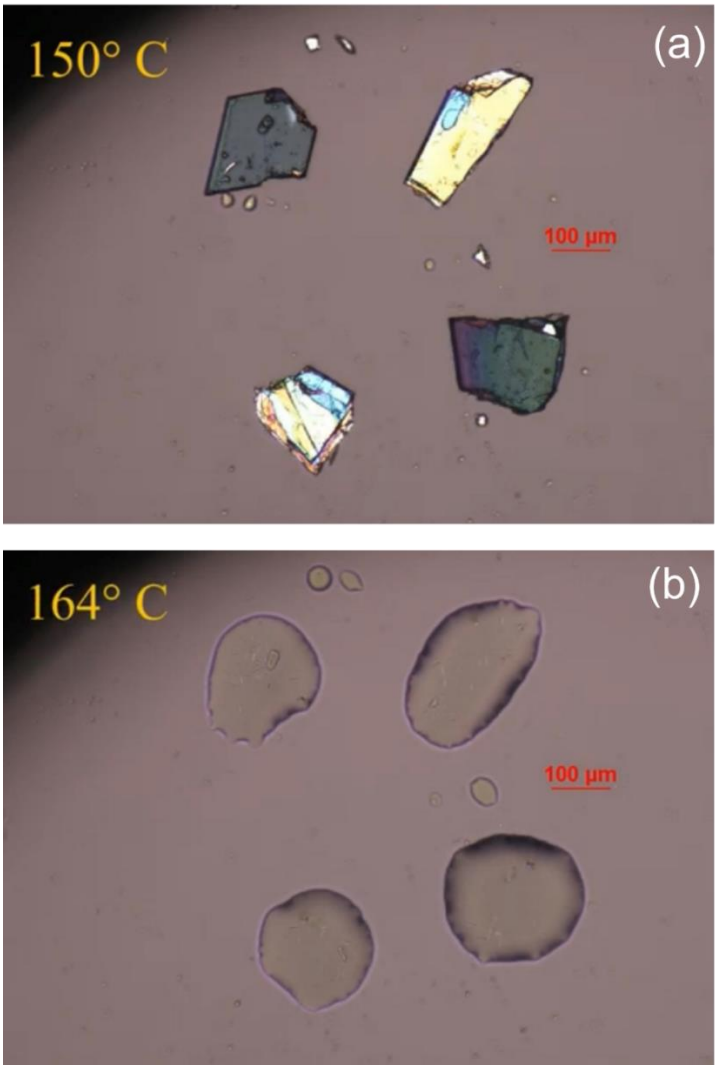

Figure 3.7 HSM to determine the melting range of Form I of Eph-Cyc; (a) initiation of melting; (b) melting completed

Video link:

https://drive.google.com/file/d/1c7e3gpuTuGAECvMJCwmRSvPJFpnq--S4/view?usp=share_link

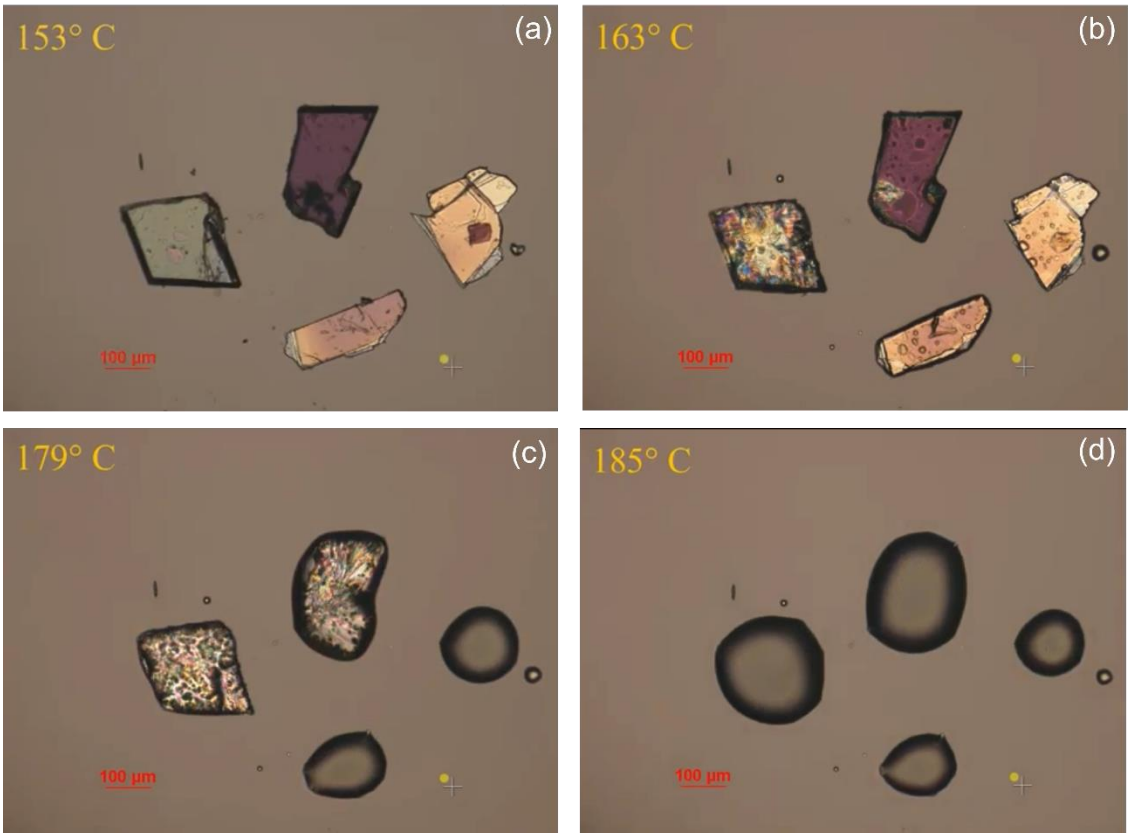

Figure 3.8 HSM images of four crystals;(a) melting begins for two crystals; (b)two crystals undergo transformation; (c) Form I crystals have melted completely; (d) melting of Form II

Video link:

https://drive.google.com/file/d/18RfH2_Hglx_jvzii2Zu0Kt_5wdilHBKG/view?usp=share_link

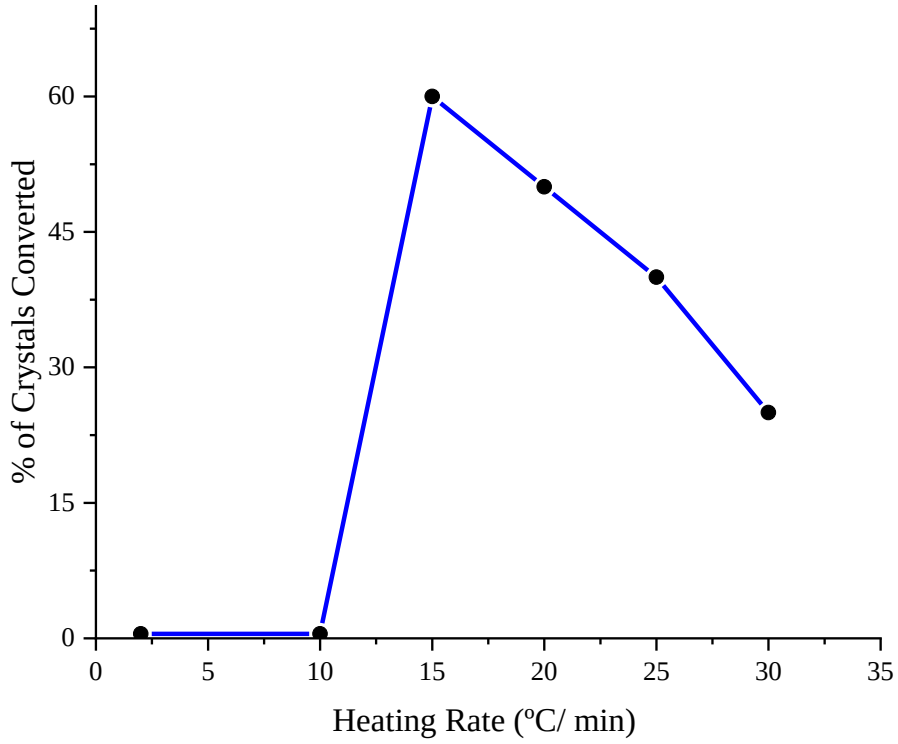

Figure 3.9 Phase conversion of Eph-Cyc based on the heating rate.

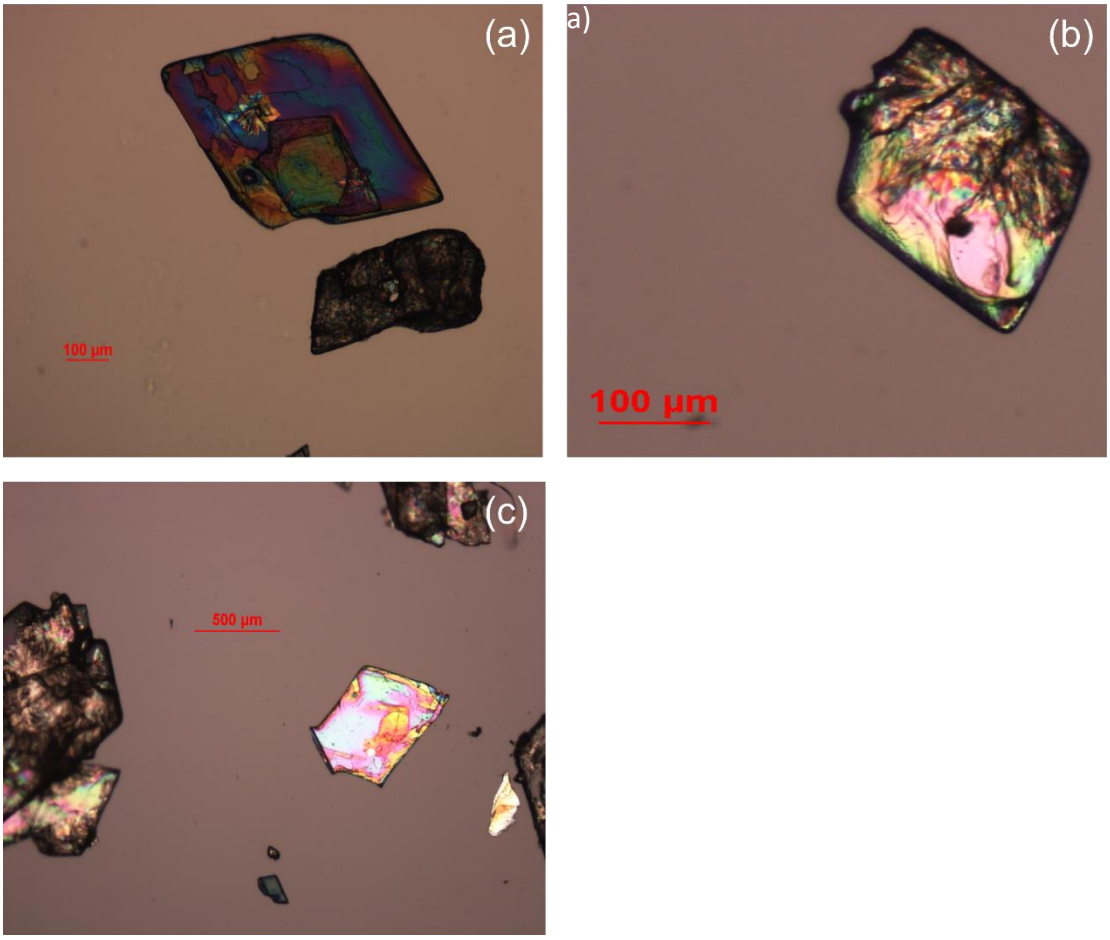

Figure 3.10 Microscopic images of crystals obtained from TGA; (a,b) crystals stuck in mid-transformation; (c) untransformed crystal (bright pink) along with degenerated crystals (left)

Chapter 4

RESEARCH SUMMARY AND FUTURE WORK

4.1 Research Summary

A 1:1 salt of ephedrine cyclamate and sodium cyclamate was successfully prepared and characterized. Eph-Cyc has improved tabletability and plasticity than its parent salts. Eph-Cyc also has much lower hygroscopicity than ephedrine free-base. Two enantiotropic polymorphs of this salt were observed. However, bulk form II could not be produced using various thermal methods to simulate a DSC experiment.

4.2 Future Work

Given the difficulty with preparing phase pure form II of Eph-Cyc bulk powders using various thermal techniques, other crystallization techniques should be tried to produce form II, like seeding. One attempt at obtaining form II could be to extract the DSC sample after heating it to 175 °C using a pinhole or crimped lid. However, it would require multiple runs to extract even 50 mg of phase pure sample of form II. The underlying mechanism behind the unpredictive nature of transformation should be further investigated. If the production of Form II is successful, then it is possible that the crystal structure of Form II can explain the mechanism of the unique behavior of polymorphic transformation of this compound. When a bulk form II powder is obtained, the mechanical properties of both forms should be compared. Additionally, the expected taste improvement of Eph-Cyc could also be confirmed using a taste- panel.

REFERENCES

1. Wang C, Sun CC. The efficient development of a sildenafil orally disintegrating tablet using a material sparing and expedited approach. *Int J Pharm*. 2020;589. doi:10.1016/j.ijpharm.2020.119816

2. Rathbone MJ, Hadgraft J, Roberts MS. *Modified-Release Drug Delivery Technology*. Marcel Dekker; 2003.

3. Kalepu S, Nekkanti V. Insoluble drug delivery strategies: Review of recent advances and business prospects. *Acta Pharm Sin B*. 2015;5(5):442-453. doi:10.1016/j.apsb.2015.07.003

4. Loftsson T, Brewster ME. Pharmaceutical applications of cyclodextrins: Basic science and product development. *Journal of Pharmacy and Pharmacology*. 2010;62(11):1607-1621. doi:10.1111/j.2042-7158.2010.01030.x

5. Desiraju GR, Parshall GW. Crystal engineering: the design of organic solids. *Materials science monographs*. 1989;54.

6. Vishweshwar P, McMahon JA, Peterson ML, Hickey MB, Shattock TR, Zaworotko MJ. Crystal engineering of pharmaceutical co-crystals from polymorphic active pharmaceutical ingredients. *Chemical Communications*. 2005;(36):4601-4603. doi:10.1039/b501304f

7. Reddy DS, Ovchinnikov YE, Shishkin O V, Struchkov YT, Desiraju GR. Supramolecular synthons in crystal engineering. 3. Solid state architecture and synthon robustness in some 2, 3-dicyano-5, 6-dichloro-1, 4-dialkoxybenzenes1. *J Am Chem Soc*. 1996;118(17):4085-4089.

8. Dissertation A, Liang Z, Sun CC. *Discovery, Characterization, and Pharmaceutical Applications of Two Loratadine-Oxalic Acid Cocrystals*.; 2020.

9. Chattoraj S, Shi L, Sun CC. Understanding the relationship between crystal structure, plasticity and compaction behaviour of theophylline, methyl gallate, and their 1: 1 co-crystal. *CrystEngComm*. 2010;12(8):2466-2472.

10. Sun CC, Hou H. Improving mechanical properties of caffeine and methyl gallate crystals by cocrystallization. *Cryst Growth Des*. 2008;8(5):1575-1579.

11. Reddy CM, Krishna GR, Ghosh S. Mechanical properties of molecular crystals—applications to crystal engineering. *CrystEngComm*. 2010;12(8):2296-2314.

12. Schultheiss N, Newman A. Pharmaceutical cocrystals and their physicochemical properties. *Cryst Growth Des*. 2009;9(6):2950-2967.

13. Liu S, Sun CC. *SWEET SULFAMETHAZINE ACESULFAMATE CRYSTALS WITH IMPROVED COMPACTION PROPERTY A DISSERTATION SUBMITTED TO THE FACULTY OF UNIVERSITY OF MINNESOTA BY*.; 2019.

14. Fu X, Li J, Wang L, et al. Pharmaceutical crystalline complexes of sulfamethazine with saccharin: same interaction site but different ionization states. *RSC Adv*. 2016;6(31):26474-26478.

15. Sun CC, Davé RN. Crystal and Particle Engineering – An Indispensable Tool for Developing and Manufacturing Quality Pharmaceutical Products. *Pharm Res*. 2022;39(12):3041-3045. doi:10.1007/s11095-022-03449-x

16. Chattoraj S, Sun CC. Crystal and Particle Engineering Strategies for Improving Powder Compression and Flow Properties to Enable Continuous Tablet Manufacturing by Direct Compression. *J Pharm Sci*. 2018;107(4):968-974. doi:10.1016/j.xphs.2017.11.023

17. Blagden N, de Matas M, Gavan PT, York P. Crystal engineering of active pharmaceutical ingredients to improve solubility and dissolution rates. *Adv Drug Deliv Rev*. 2007;59(7):617-630.

18. Sun CC. Cocrystallization for successful drug delivery. *Expert Opin Drug Deliv*. 2013;10(2):201-213. doi:10.1517/17425247.2013.747508

19. Administration USF and D. Guidance for industry: Regulatory classification of pharmaceutical co-crystals. *Center for Drug Evaluation and Research, Silver Spring, US*. Published online 2013.

20. Berge SM, Bighley LD, Monkhouse DC. *Pharmaceutical Salts and Organoleptic Properties of Pharmaceutical Salts, Review Bioavailability-Formulation Effects, Absorption Alteration and Phar-Macokinetics of Pharmaceutical Salts, Review 0 Toxicology-Pharma-Ceutical Salts, Review CONTENTS*. Vol 66.; 1977.

21. Cruz-Cabeza AJ. Acid–base crystalline complexes and the p K a rule. *CrystEngComm*. 2012;14(20):6362-6365.

22. Childs SL, Stahly GP, Park A. The salt− cocrystal continuum: the influence of crystal structure on ionization state. *Mol Pharm*. 2007;4(3):323-338.

23. Cruz-Cabeza AJ. Acid–base crystalline complexes and the p K a rule. *CrystEngComm*. 2012;14(20):6362-6365.

24. Stahl PH, Wermuth CG. Handbook of pharmaceutical salts: properties, selection and use. *Chem Int*. 2002;24:21.

25. Li ZJ, Abramov Y, Bordner J, Leonard J, Medek A, Trask A V. Solid-state acid− base interactions in complexes of heterocyclic bases with dicarboxylic acids: crystallography, hydrogen bond analysis, and 15N NMR spectroscopy. *J Am Chem Soc*. 2006;128(25):8199-8210.

26. Steiner T, Majerz I, Wilson CC. First OHN Hydrogen Bond with a Centered Proton Obtained by Thermally Induced Proton Migration. *Angew Chem Int Ed Engl*. 2001;40(14):2651-2654.

27. Nehm SJ, Rodríguez-Spong B, Rodríguez-Hornedo N. Phase solubility diagrams of cocrystals are explained by solubility product and solution complexation. *Cryst Growth Des*. 2006;6(2):592-600.

28. Bethune SJ, Huang N, Jayasankar A, Rodriguez-Hornedo N. Understanding and predicting the effect of cocrystal components and pH on cocrystal solubility. *Cryst Growth Des*. 2009;9(9):3976-3988.

29. Zhao X, Li Q, Wang C, Hu S, He X, Sun CC. Simultaneous taste-masking and oral bioavailability enhancement of Ligustrazine by forming sweet salts. *Int J Pharm*. 2020;577:119089.

30. Wang C, Perumalla SR, Lu R, Fang J, Sun CC. Sweet berberine. *Cryst Growth Des*. 2016;16(2):933-939.

31. Zhou Q, Peng Z, Huang X. Establishment of a Stable Acute Drug-Induced Liver Injury Mouse Model by Sodium Cyclamate. *J Inflamm Res*. 2022;15:1599-1615. doi:10.2147/JIR.S354273

32. Jamilatun M, Lukito PI, Astuti ID. Sodium Cyclamate Identification and Determination of Dawet Ice Sold in Wedi District Indonesia. *Food ScienTech Journal*. 2022;4(1):69. doi:10.33512/fsj.v4i1.14206

33. Number CAS. Dietary supplements. *History*. 7440:70-72.

34. Smith J, Hong-Shum L. *Food Additives Data Book*. John Wiley & Sons; 2011.

35. Ashurst PR. *Chemistry and Technology of Soft Drinks and Fruit Juices*. John Wiley & Sons; 2016.

36. Dikötter F, Laamann LP, Xun Z. *Narcotic Culture: A History of Drugs in China*. Hong Kong University Press; 2004.

37. Refat MS, Ibrahim OB, Saad HA, Adam AMA. Usefulness of charge-transfer complexation for the assessment of sympathomimetic drugs: Spectroscopic properties of

drug ephedrine hydrochloride complexed with some π-acceptors. *J Mol Struct*. 2014;1064(1):58-69. doi:10.1016/j.molstruc.2014.02.024

38. Ford MD, Delaney K, Erickson TB. *Clinical Toxicology*. WB Saunders Company; 2001.

39. Miller NS. *Principles of Addictions and the Law: Applications in Forensic, Mental Health, and Medical Practice*. Academic Press; 2010.

40. Patil PN, Tye A, LaPidus JB. A pharmacological study of the ephedrine isomers. *Journal of Pharmacology and Experimental Therapeutics*. 1966;151(2):330.

41. Budavari S, O'Neil MJ, Heckelman PE. The merck index an encyclopedia of chemical, drugs, and biologicals. In: *The Merck Index an Encyclopedia of Chemical, Drugs, and Biologicals*. Merck & Co; 1989.

42. Mathew M, Palenik GJ. The crystal and molecular structures of (+)-pseudoephedrine and (+)-pseudoephedrine hydrochloride. *Acta Crystallogr B*. 1977;33(4):1016-1022. doi:10.1107/s0567740877005287

43. Bernstein J. Polymorphism− a perspective. *Cryst Growth Des*. 2011;11(3):632-650.

44. Kuhnert-Brandstatter M. . *Pharm Z*. 1975;4:131-137.

45. Roy R. Classification of non-crystalline solids. *J Non Cryst Solids*. 1970;3(1):33-40.

46. Klug HP, Alexander LE. *X-Ray Diffraction Procedures: For Polycrystalline and Amorphous Materials*.; 1974.

47. Dunitz JD, Bernstein J. *Disappearing Polymorphs*. Vol 28.; 1995. https://pubs.acs.org/sharingguidelines

48. Verma AR, Krishna P. Polymorphism and polytypism in crystals. *1966, 341 P JOHN WILEY AND SONS, INC, 605 THIRD AVENUE, NEW YORK, N Y 10016*. Published online 1965.

49. Nagasako Noboru. On enantiotropy and monotropy. I. Published online April 28, 1928.

50. Burger A, Ramberger R. *On the Polymorphism of Pharmaceuticals and Other Molecular Crystals. I Theory of Thermodynamic Rules*.

51. Sheldrick GM. A short history of SHELX. *Acta Crystallogr A*. 2008;64(1):112-122.

52. Vreeman G, Sun CC. Mean yield pressure from the in-die Heckel analysis is a reliable plasticity parameter. *Int J Pharm X*. 2021;3:100094. doi:https://doi.org/10.1016/j.ijpx.2021.100094

53. Good DJ, Rodriguez-Hornedo N. Solubility advantage of pharmaceutical cocrystals. *Cryst Growth Des*. 2009;9(5):2252-2264.

54. Sun CC. Materials science tetrahedron—A useful tool for pharmaceutical research and development. *J Pharm Sci*. 2009;98(5):1671-1687.

55. Cruz-Cabeza AJ. Acid–base crystalline complexes and the p K a rule. *CrystEngComm*. 2012;14(20):6362-6365.

56. Black SN, Collier EA, Davey RJ, Roberts RJ. Structure, solubility, screening, and synthesis of molecular salts. *J Pharm Sci*. 2007;96(5):1053-1068. doi:10.1002/jps.20927

57. K.D. Aparnathi KD. Chemistry and Use of Artificial Intense Sweeteners. *Int J Curr Microbiol Appl Sci*. 2017;6(6):1283-1296. doi:10.20546/ijcmas.2017.606.151

58. Sun CC, Hou H, Gao P, Ma C, Medina C, Alvarez FJ. Development of a high drug load tablet formulation based on assessment of powder manufacturability: moving towards quality by design. *J Pharm Sci*. 2009;98(1):239-247.

59. Medina DA V, Ferreira APG, Cavalheiro ETG. Polymorphism and thermal behavior of sodium cyclamate. *J Therm Anal Calorim*. 2019;137:1307-1313.